The Extragalactic Background Light in the *Fermi*-LAT era

Alberto Domínguez

Universidad Complutense de Madrid

M. Ajello, K. Helgason, J. Finke, A. Desai, V. Paliya
and also R. Wojtak, F. Prada, L. Marcotulli, D. Hartmann

Fermi-LAT Collaboration, 2018, Science, 362, 1031
Desai et al., 2019, ApJL, 874, 7
Domínguez et al., 2019, arXiv:1903.12097

Domínguez, Primack, Bell
Scientific American, June 2015

Seminar @ Institute for Cosmic-Ray Research - September 4, 2019

The Extragalactic
Backgroun
Fermi-l

Alberto

Universidad Co

M. Ajello, K. Helgason,

and also R. Wojtak, F. Pra

Fermi-LAT Collaboration,

Desai et al., 2019, ApJL, 874,

Domínguez et al., 2019, arXiv:1903.1209

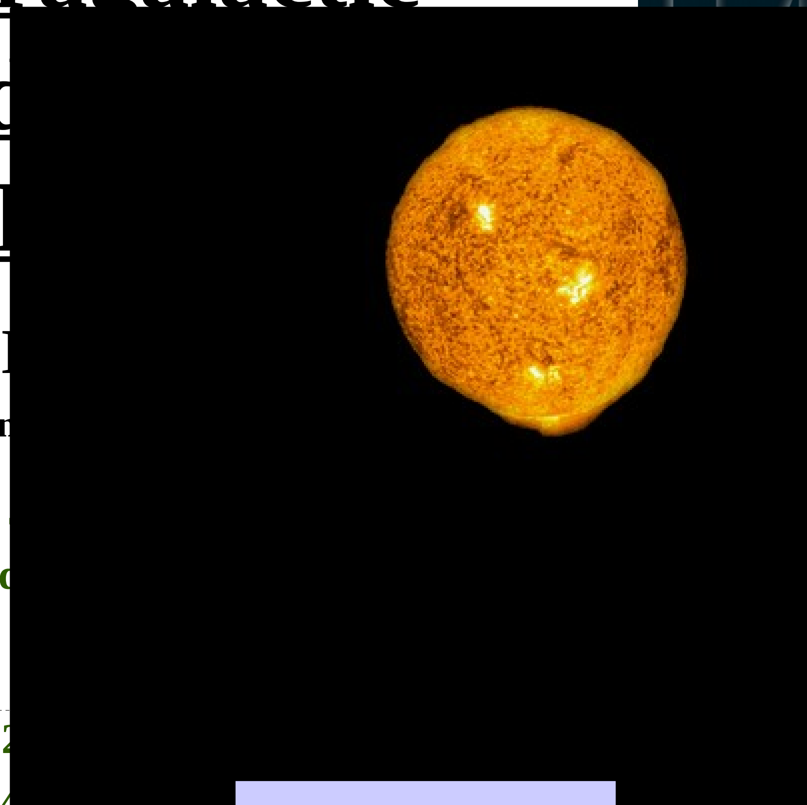

Olber's Paradox

Domínguez, Primack, Bell

Scientific American, June 2015

Seminar @ Institute for Cosmic-Ray Research - September 4, 2019

Galaxy Evolution and Cosmology

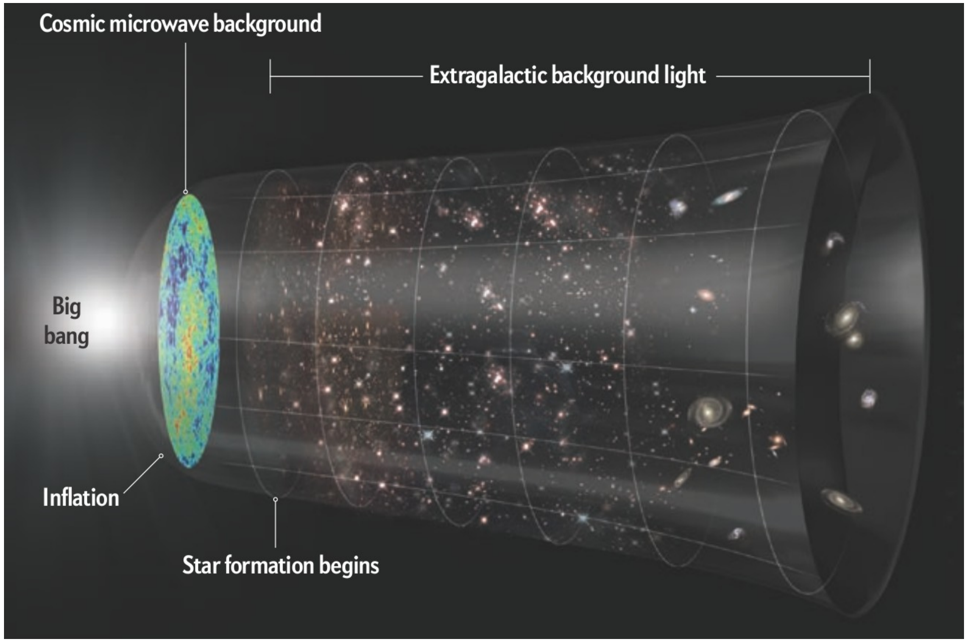

Scientific American, June 2015

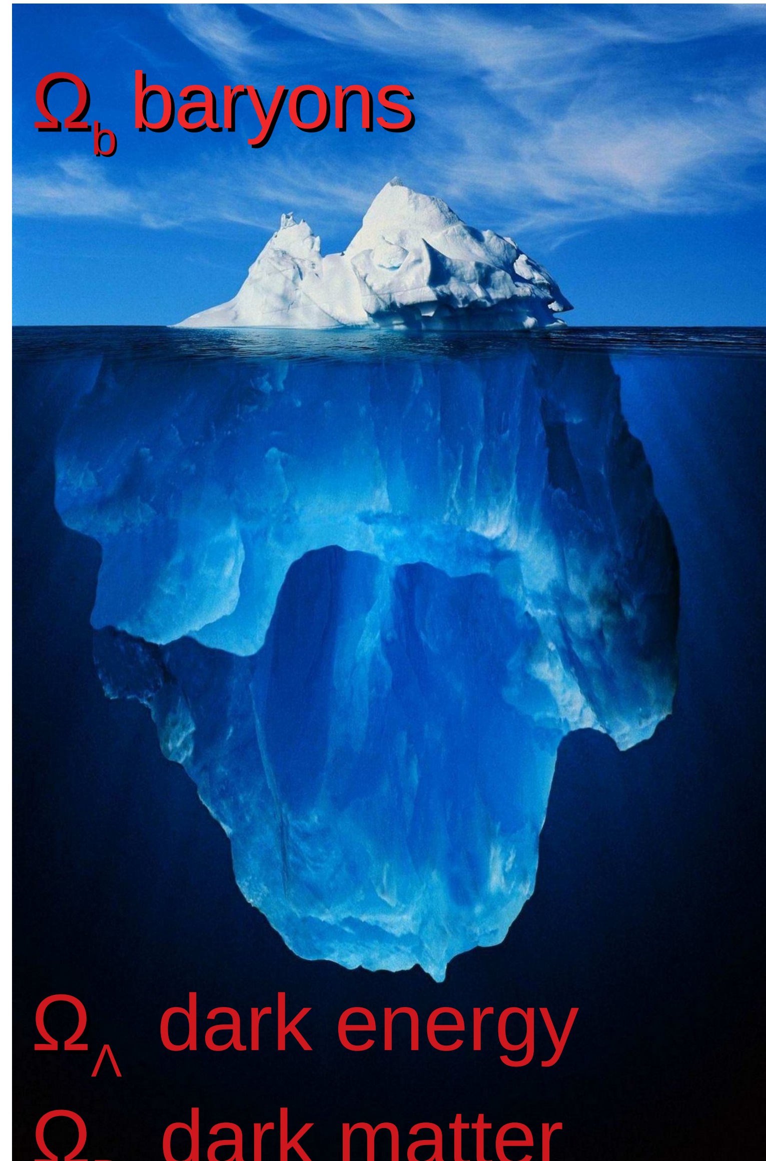

$$\Omega_m = \Omega_b + \Omega_D$$

$$\Omega_m + \Omega_\Lambda = 1$$

Cosmic Diffuse Extragalactic Backgrounds

Artistic representation of a binary system

Herschel far-IR

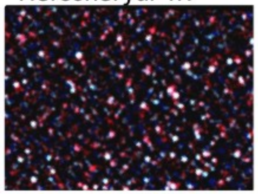

Spitzer mid-IR

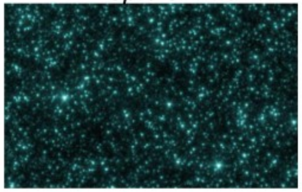

HST-optical/UV

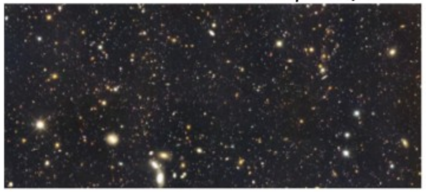

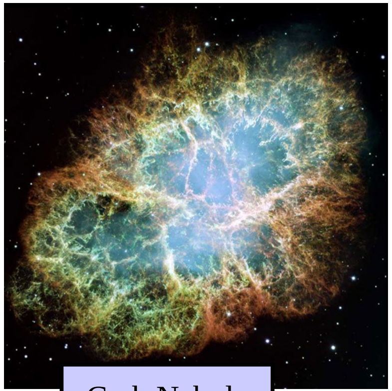

Crab Nebula

0.850-1.2mm

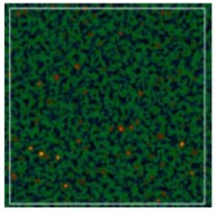

in the future: ALMA, CCAT..

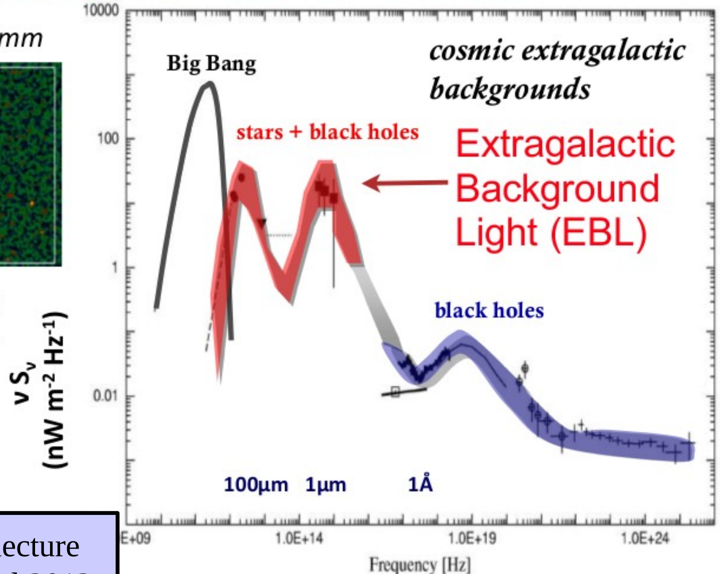

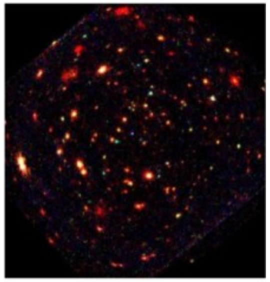

Chandra/XMM –X-ray

From Reinhard Genzel's lecture @ Jerusalem Winter School 2013

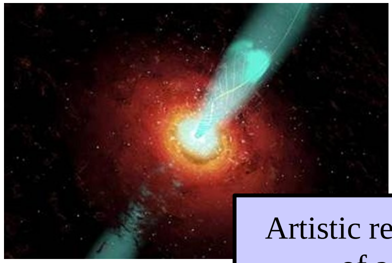

Artistic representation of a blazar

Orion Nebula (birth place of stars)

Measuring the Extragalactic Background Light

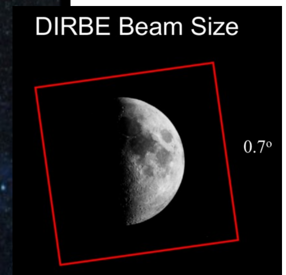

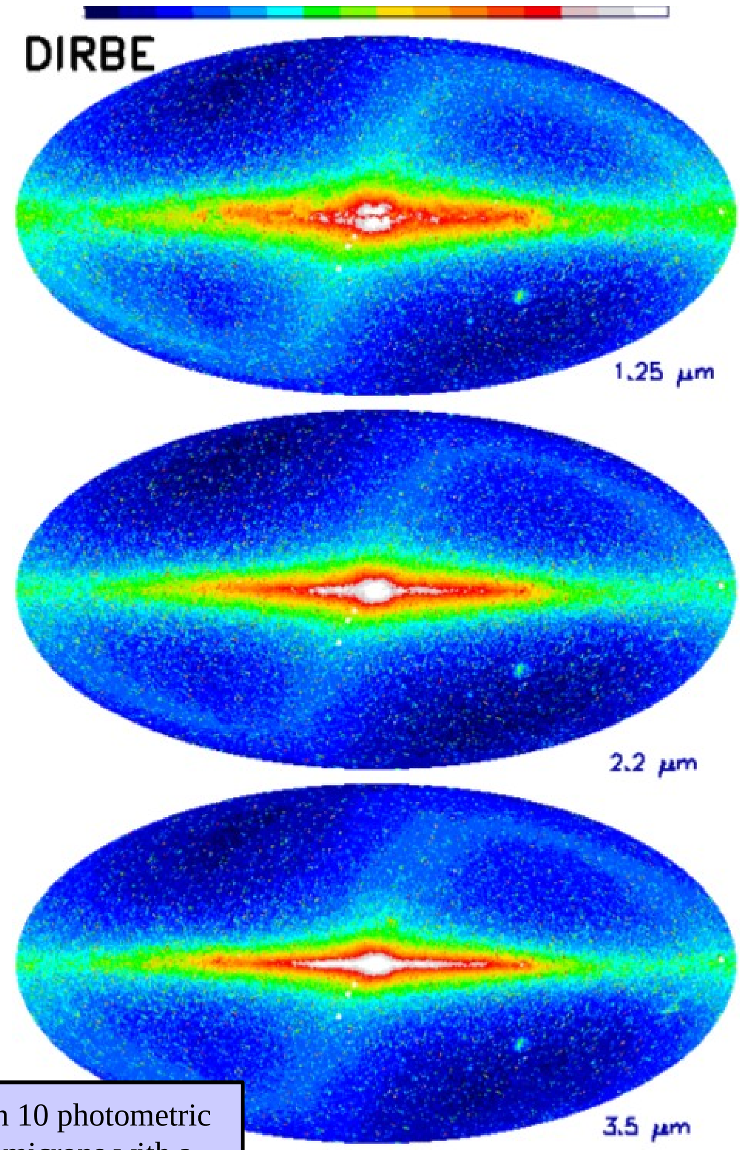

DIRBE imaged the sky in 10 photometric bands from 1.25 to 240 microns with a beam size of 0.7x0.7 sq. degrees

Measuring the Extragalactic Background Light

Zodiacal light, visible under the right conditions: typically after the sunset in Spring and right before sunrise in Autumn

TABLE 2

DECOMPOSITION OF THE DIRBE INTENSITY

Component	2.2 μm (kJy sr^{-1})	3.5 μm (kJy sr^{-1})
Total	137.5 ± 0.3	105.3 ± 0.3
Zodi	101.8 ± 3.8	80.4 ± 3.3
ISM	...	1.1 ± 0.2
Stars, $m < 9$ mag......	7.4 ± 2.2	5.3 ± 1.8
Stars, $m > 9$ mag......	11.9 ± 0.6	5.7 ± 0.3
EBL	16.4 ± 4.4	12.8 ± 3.8

EBL is an order of magnitude lower than foregrounds and subject to large systematic uncertainties, e.g. Gorjian+ 00

Measuring the Extragalactic Background Light

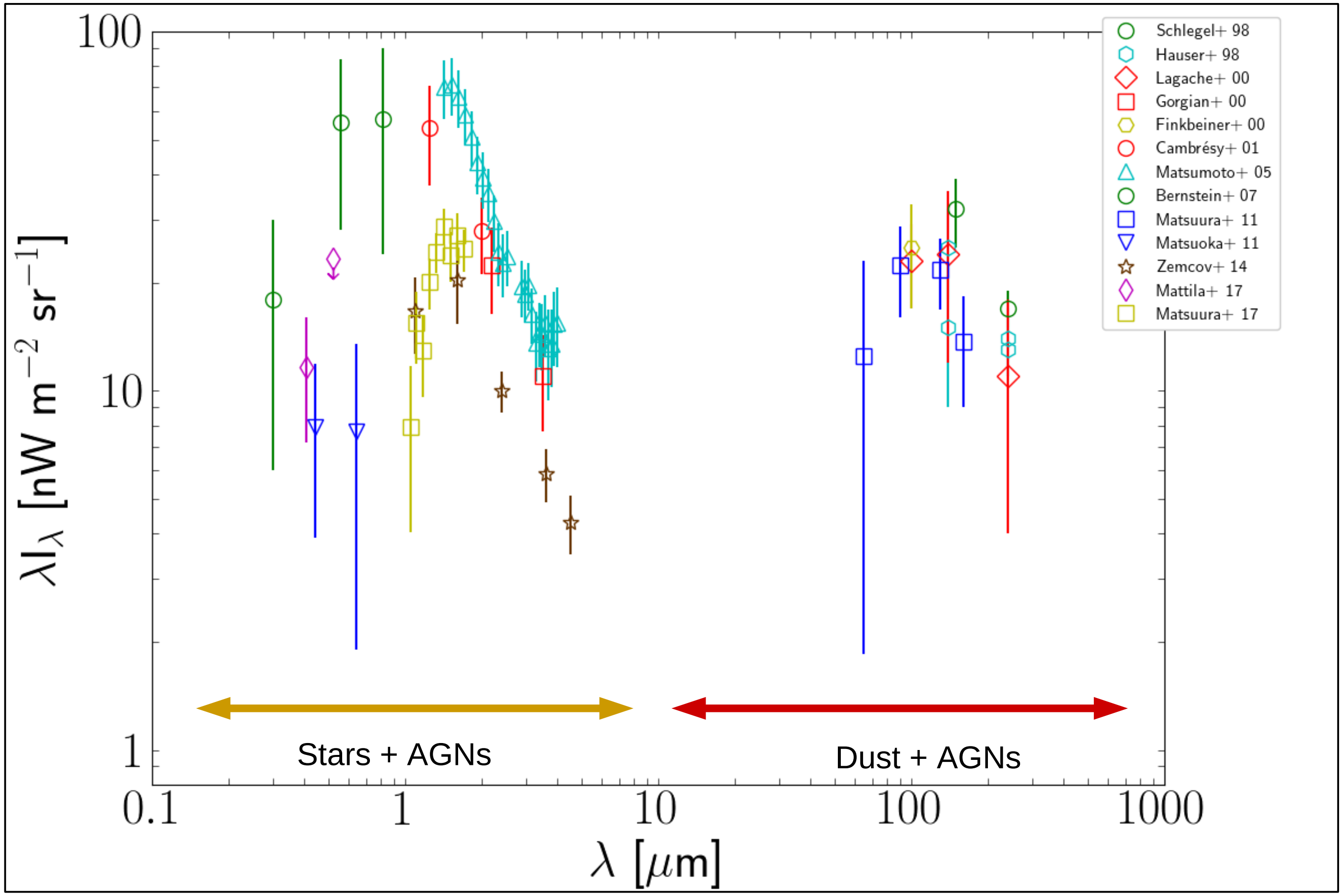

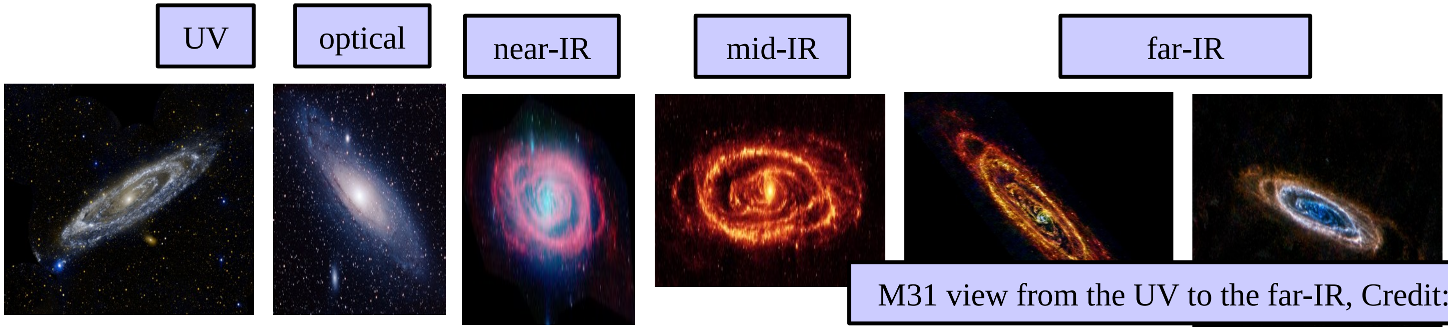

M31 view from the UV to the far-IR, Credit: NASA & ESA

Measuring the Extragalactic Background Light

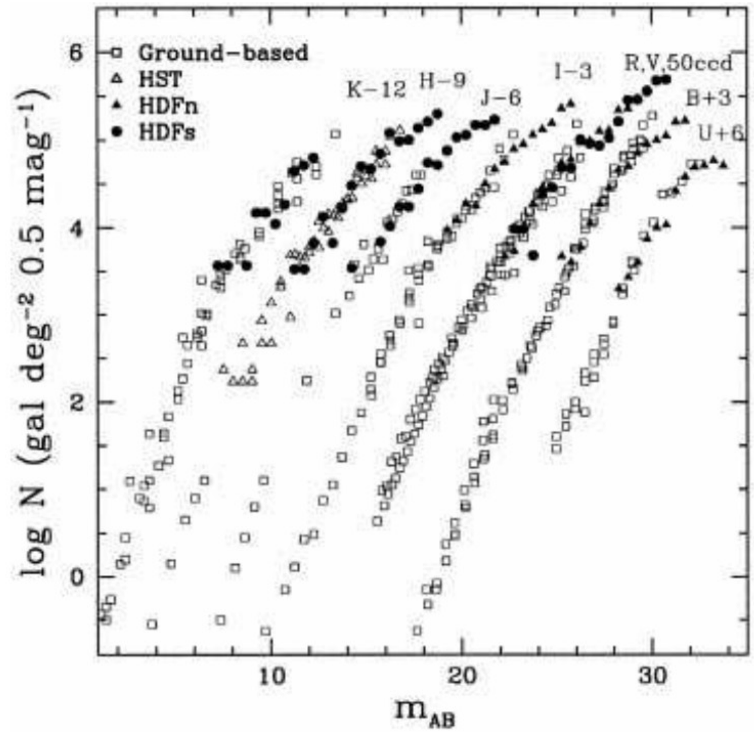

Number counts in the
Hubble Deep Field,
e.g. Madau & Pozzetti, 2000

Measuring the Extragalactic Background Light

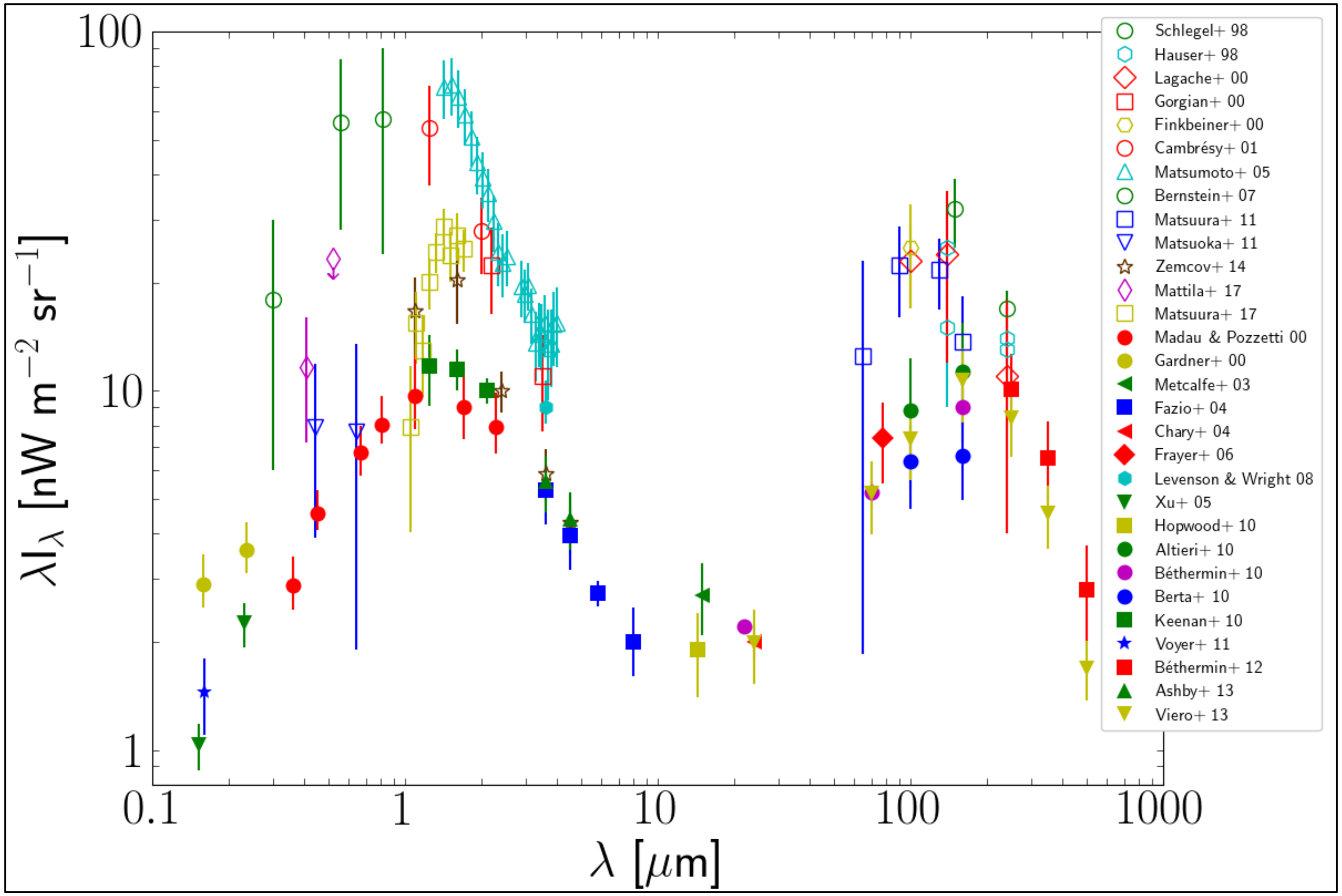

UV | optical | near-IR | mid-IR | far-IR

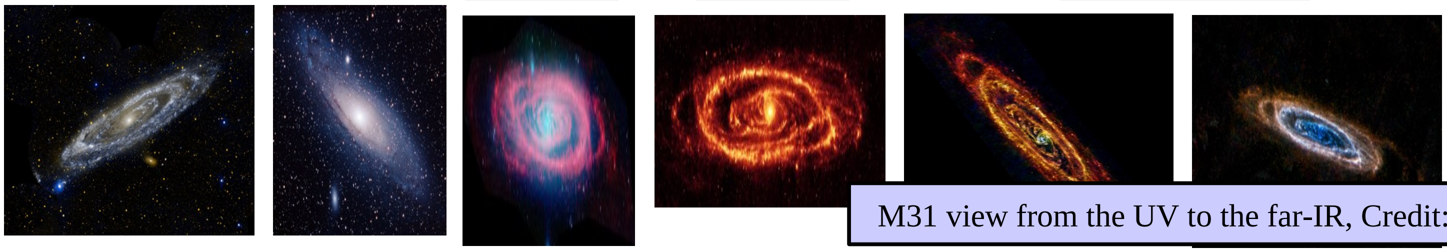

M31 view from the UV to the far-IR, Credit: NASA & ESA

Measuring the Extragalactic Background Light

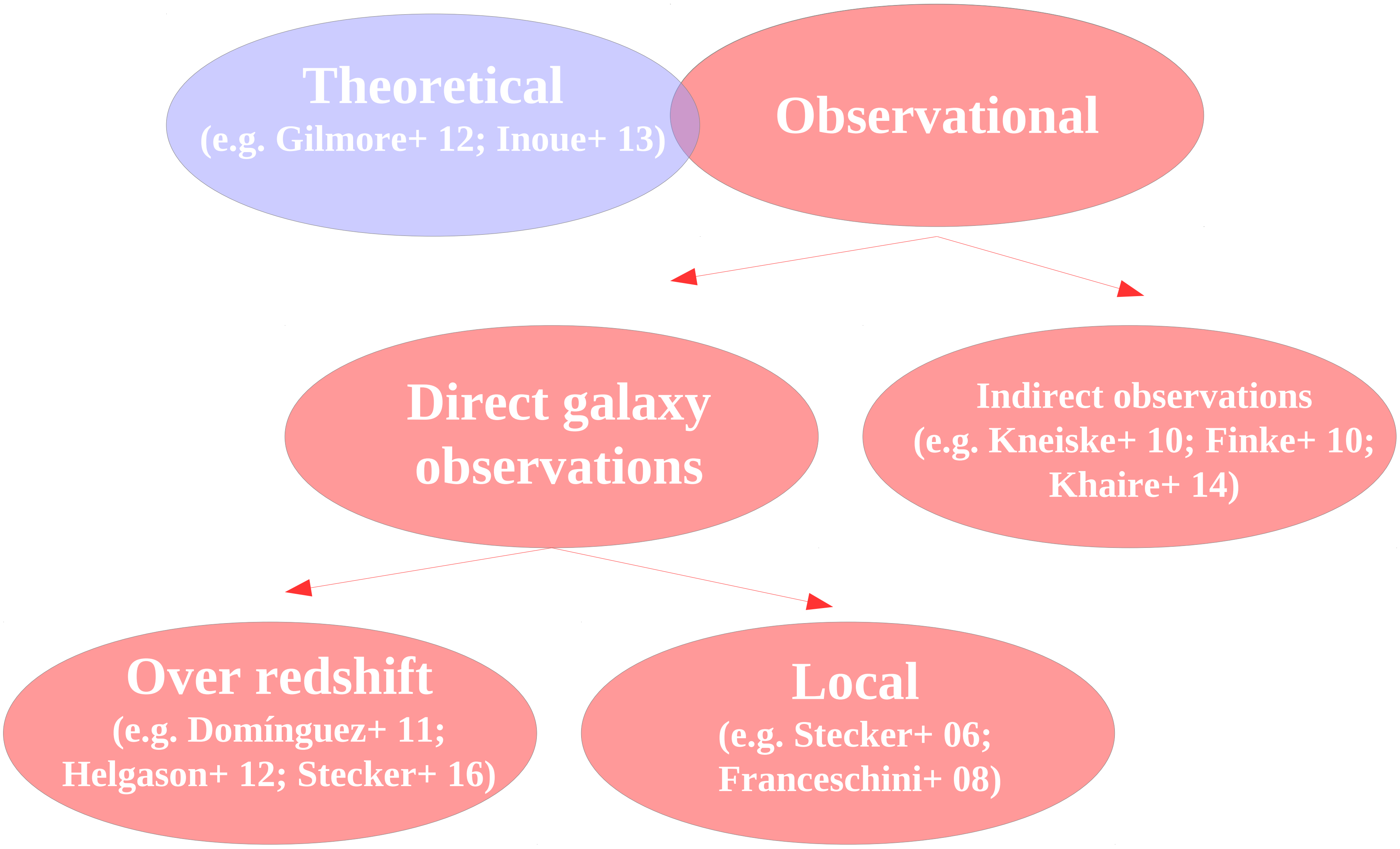

Extragalactic Background Light (Local)

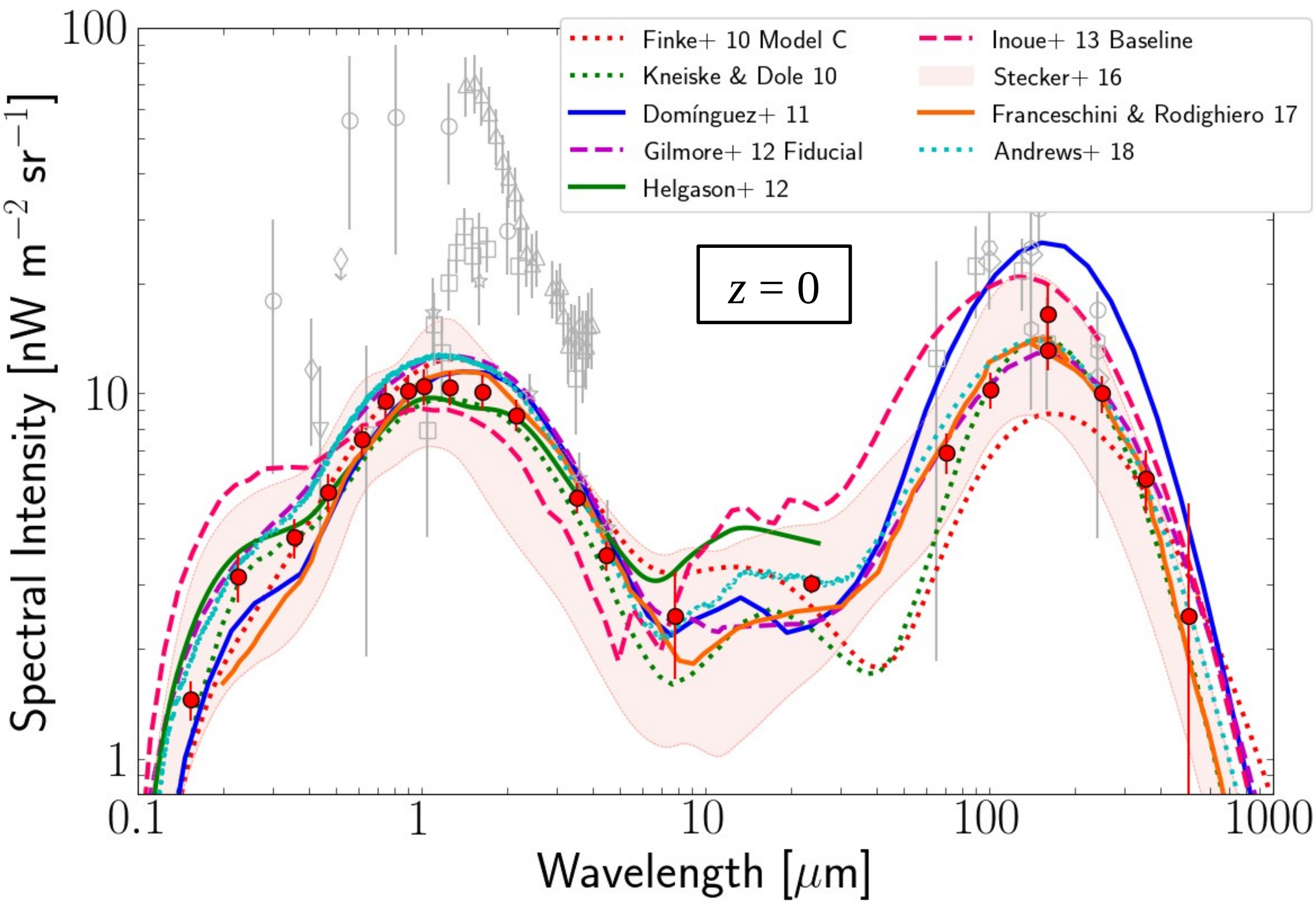

Extragalactic Background Light (Evolution)

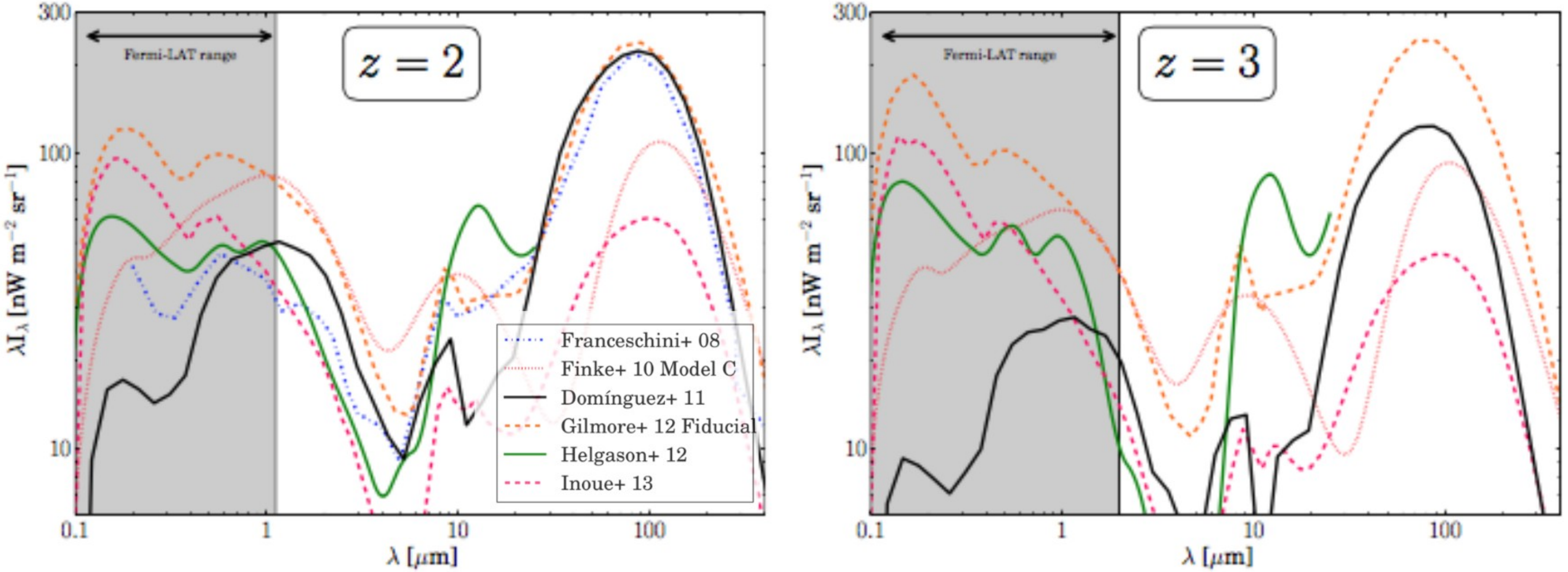

Strong divergence

Gamma-ray Attenuation

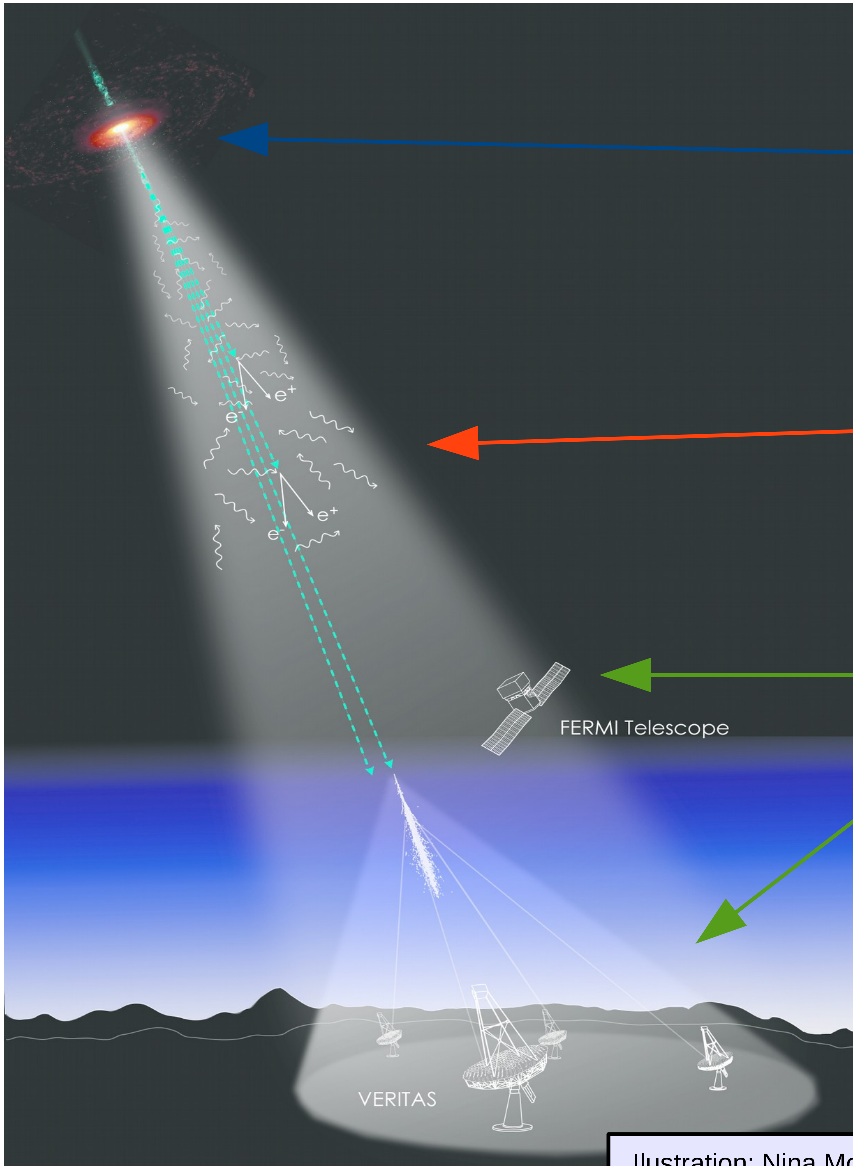

Extragalactic source:
e.g. Blazar

Blazars: AGNs emitting at all wavelength with energetic jets pointing towards us.

Pair-production interaction

Reverse of most known electron-positron annhilation process

Telescopes: Fermi-LAT and Imaging Atmospheric Cherenkov Telescopes (IACTs)

Ilustration: Nina McCurdy & Joel Primack

Gamma-ray Attenuation

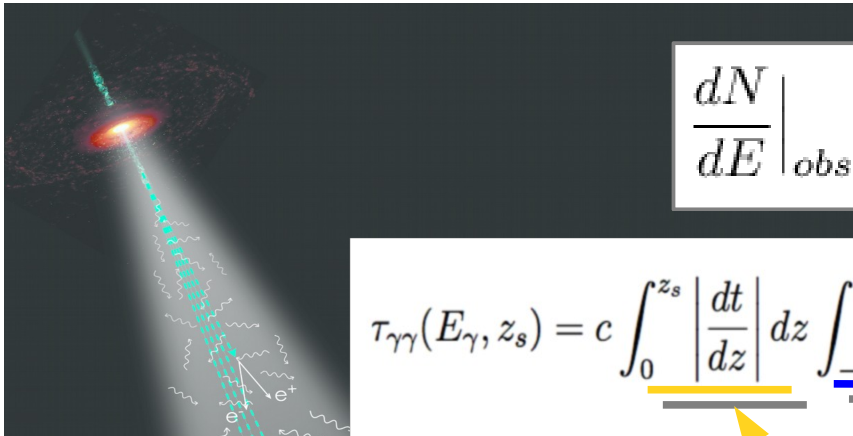

$$\left.\frac{dN}{dE}\right|_{obs} = \left.\frac{dN}{dE}\right|_{int} \exp\left[-\tau(E,z)\right]$$

$$\tau_{\gamma\gamma}(E_\gamma, z_s) = c \underbrace{\int_0^{z_s} \left|\frac{dt}{dz}\right| dz}_{\text{distance}} \underbrace{\int_{-1}^{1} (1-\mu)\frac{d\mu}{2} \int_{2m_e^2c^4/\epsilon_\gamma(1-\mu)}^{\infty} \sigma(\epsilon_{\rm EBL}, \epsilon_\gamma, \mu)}_{\text{cross section}} \underbrace{n_{\rm EBL}(\epsilon, z) d\epsilon_{\rm EBL}}_{\text{EBL photon density evolution}}$$

$$n_{\rm EBL}(\epsilon, z) = (1+z)^3 \int_z^{\infty} \frac{j(\epsilon, z)}{\epsilon} \left|\frac{dt}{dz'}\right| dz'$$

distance

cross section

EBL photon density evolution

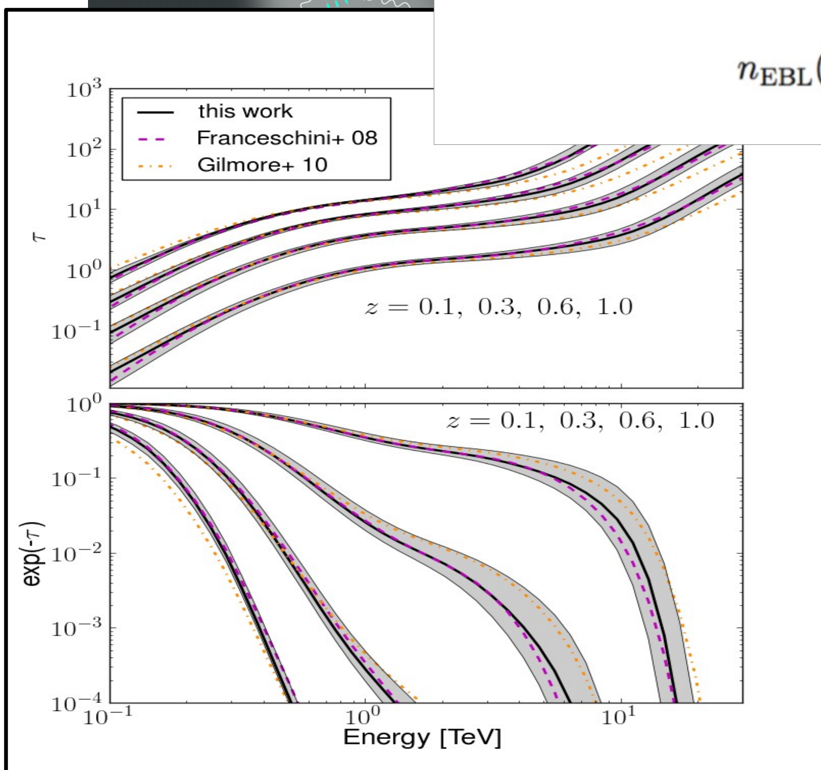

: Nina McCurdy & Joel Primack

Gamma-ray Telescopes

Fermi-LAT

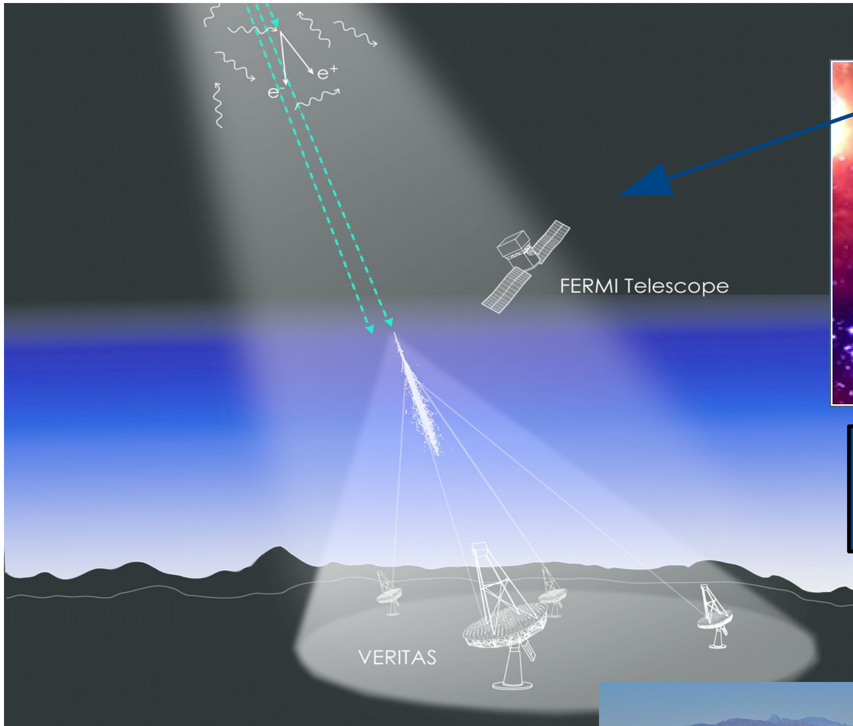

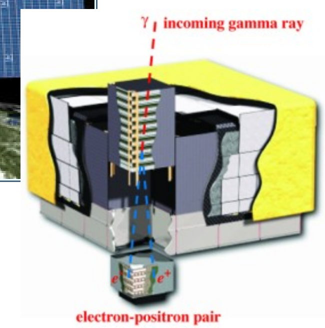

All-sky, Energy range
100 MeV – 100 GeV

IACTs
Small field of view, High sensitivity, Energy range
100 GeV – 10s TeV

CTA North, La Palma (Spain)

VERITAS, Arizona (USA)

H.E.S.S., Namibia

MAGIC, La Palma (Spain)

Gamma-ray Cherenkov Telescopes (IACTs)

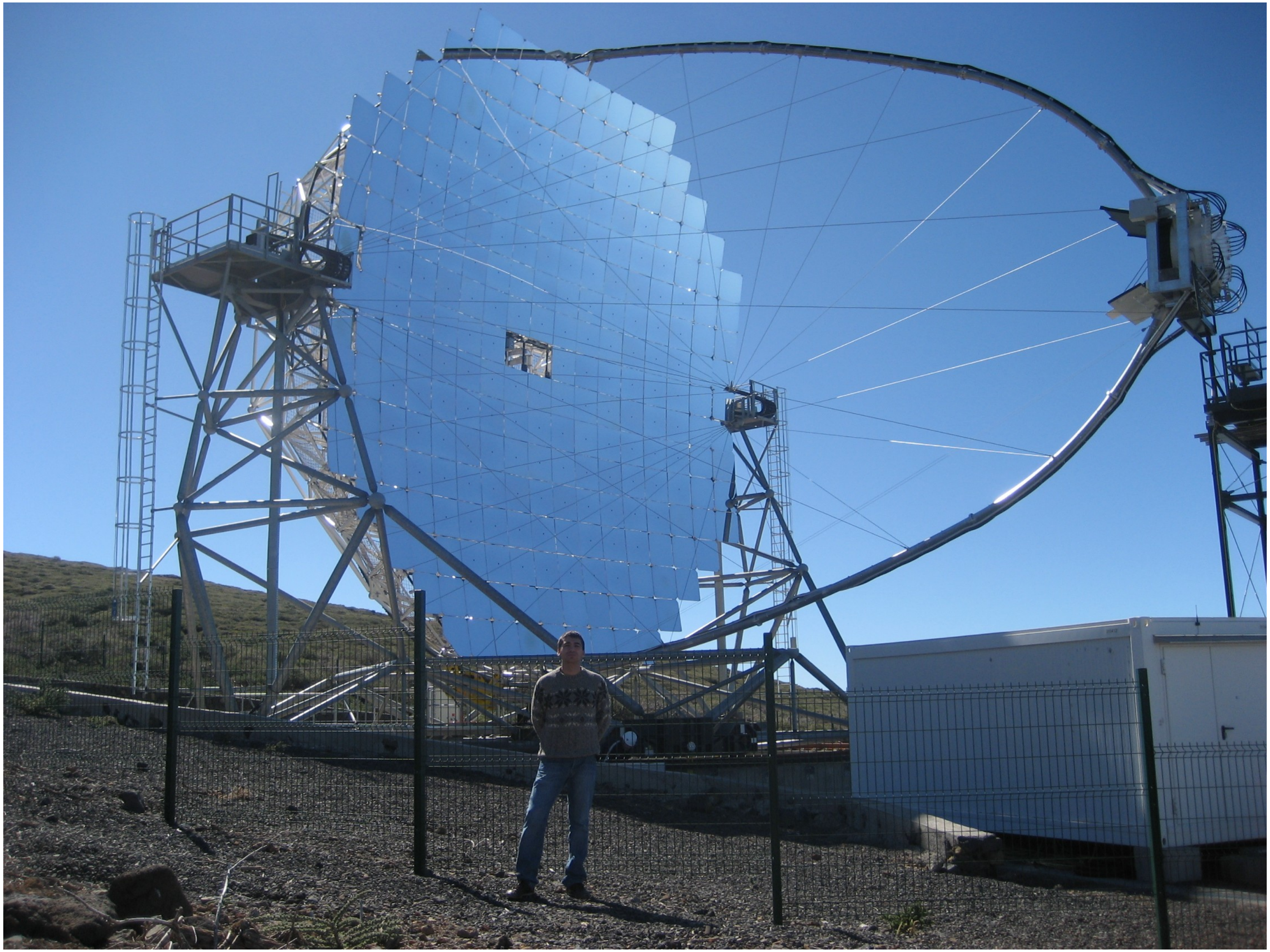

Gamma-ray Cherenkov Telescopes (IACTs)

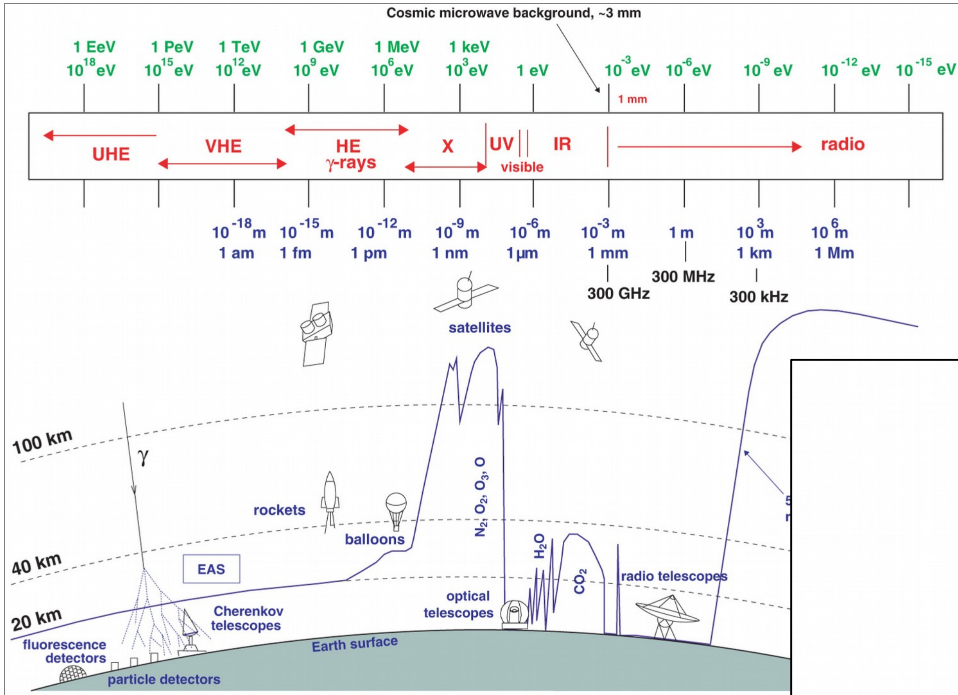

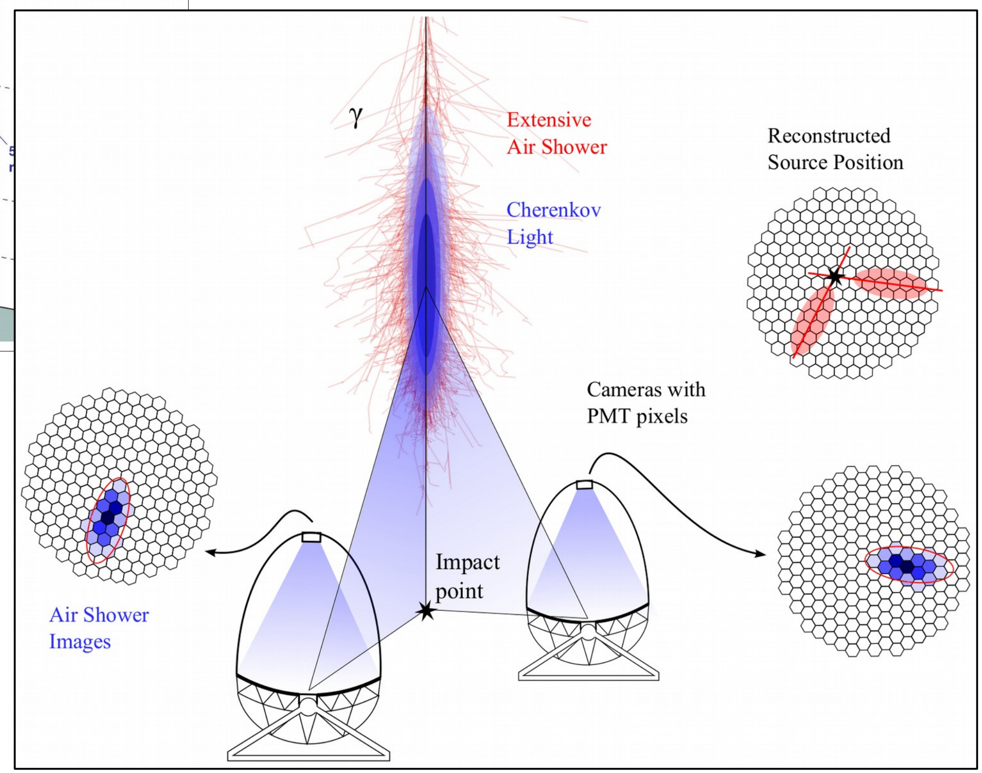

Gamma-ray Cherenkov Telescopes (IACTs)

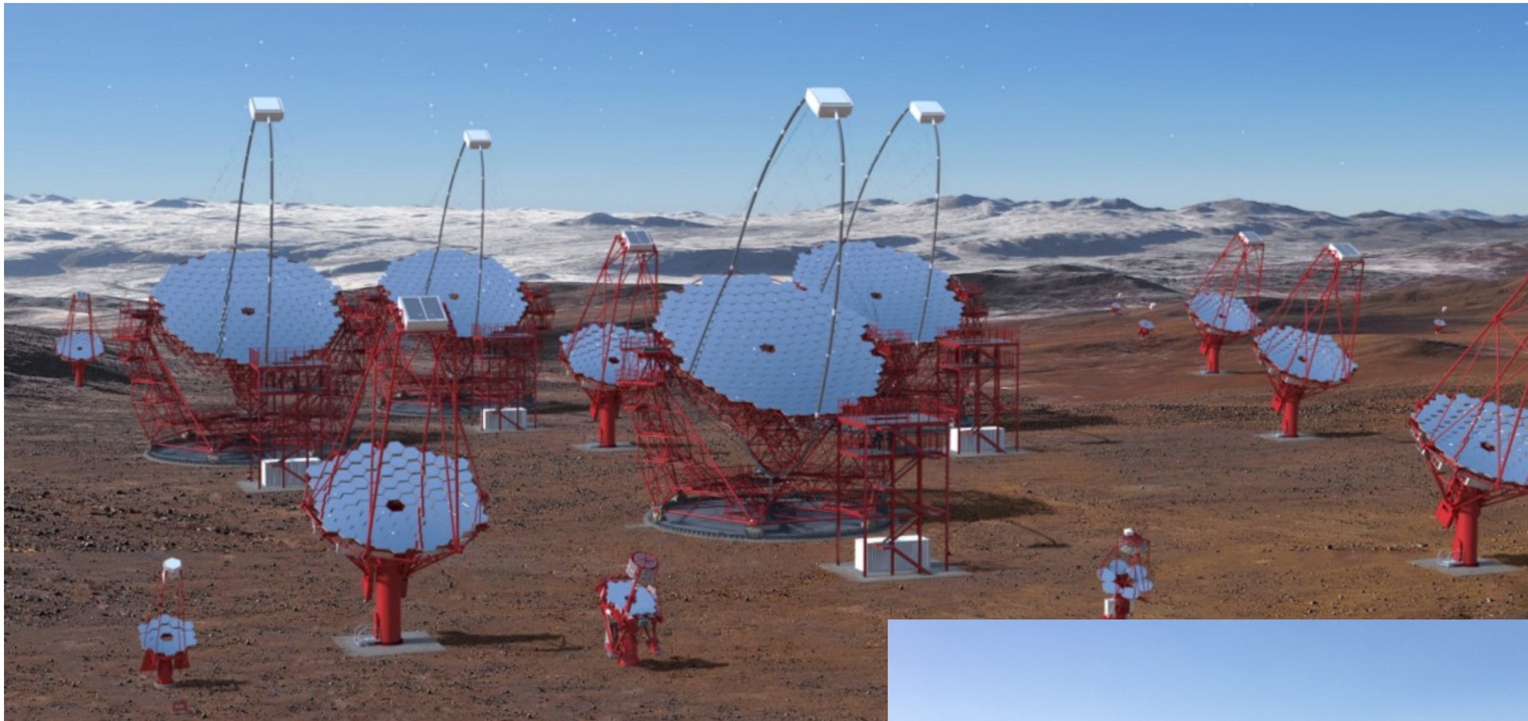

NASA's Fermi Gamma-Ray Space Telescope

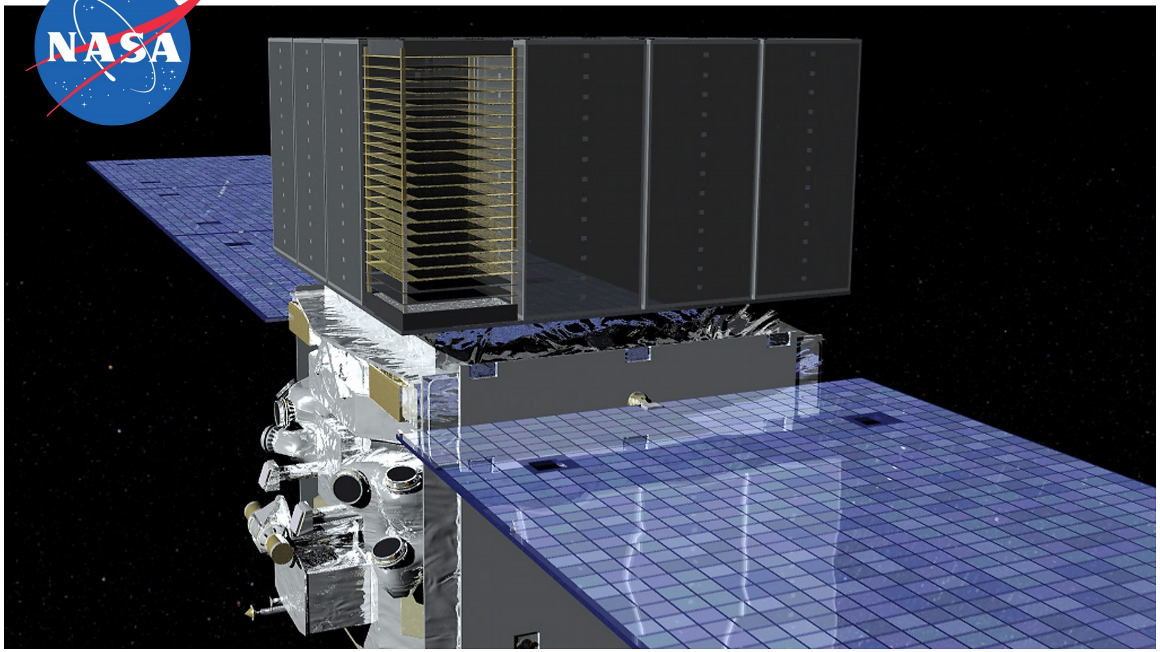

Launch June 11, 2008
Celebrating
10th year Anniversary

1. Tracking system:

- convert an incident gamma-ray to an electron-positron pair
- reconstruct the gamma-ray direction from the tracks of the pair

2. Calorimeter:

- measure the photon energy

3. Anti-coincidence detector:

- limit the cosmic-ray background

- Wide field of view (2.4 sr, 20% of the sky)
- Large effective area (~0.9 m^2 above 1 GeV)
- Low dead time (~27 μs)

The Gamma-Ray Sky

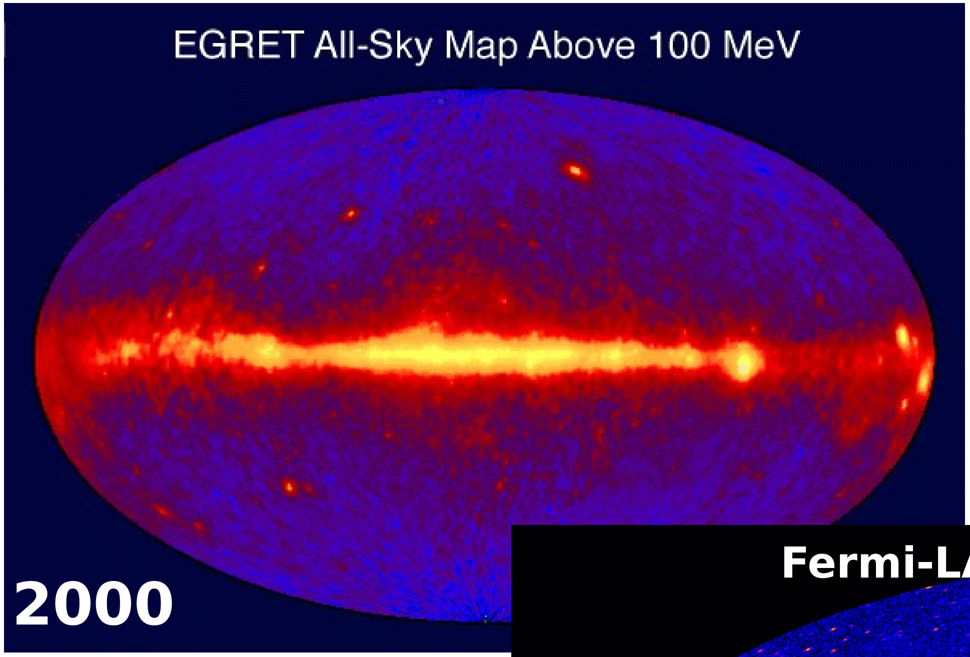

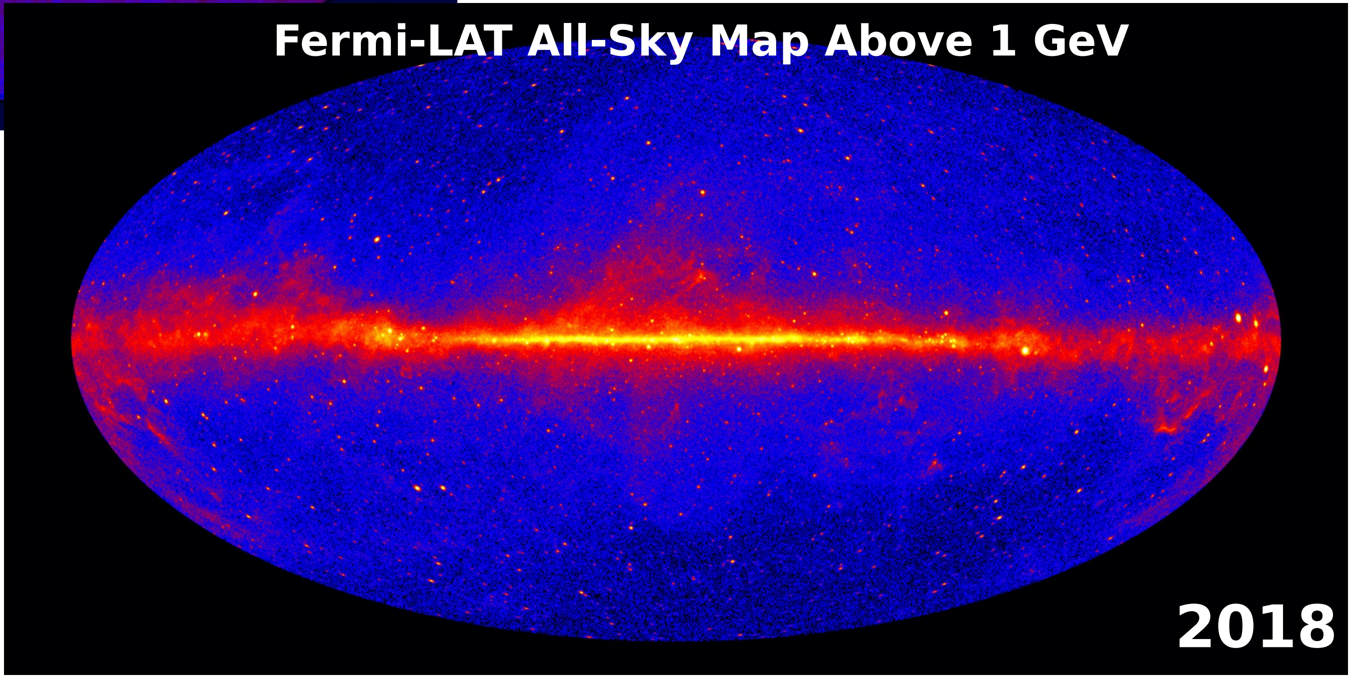

Gamma-ray Fermi-LAT Catalogs

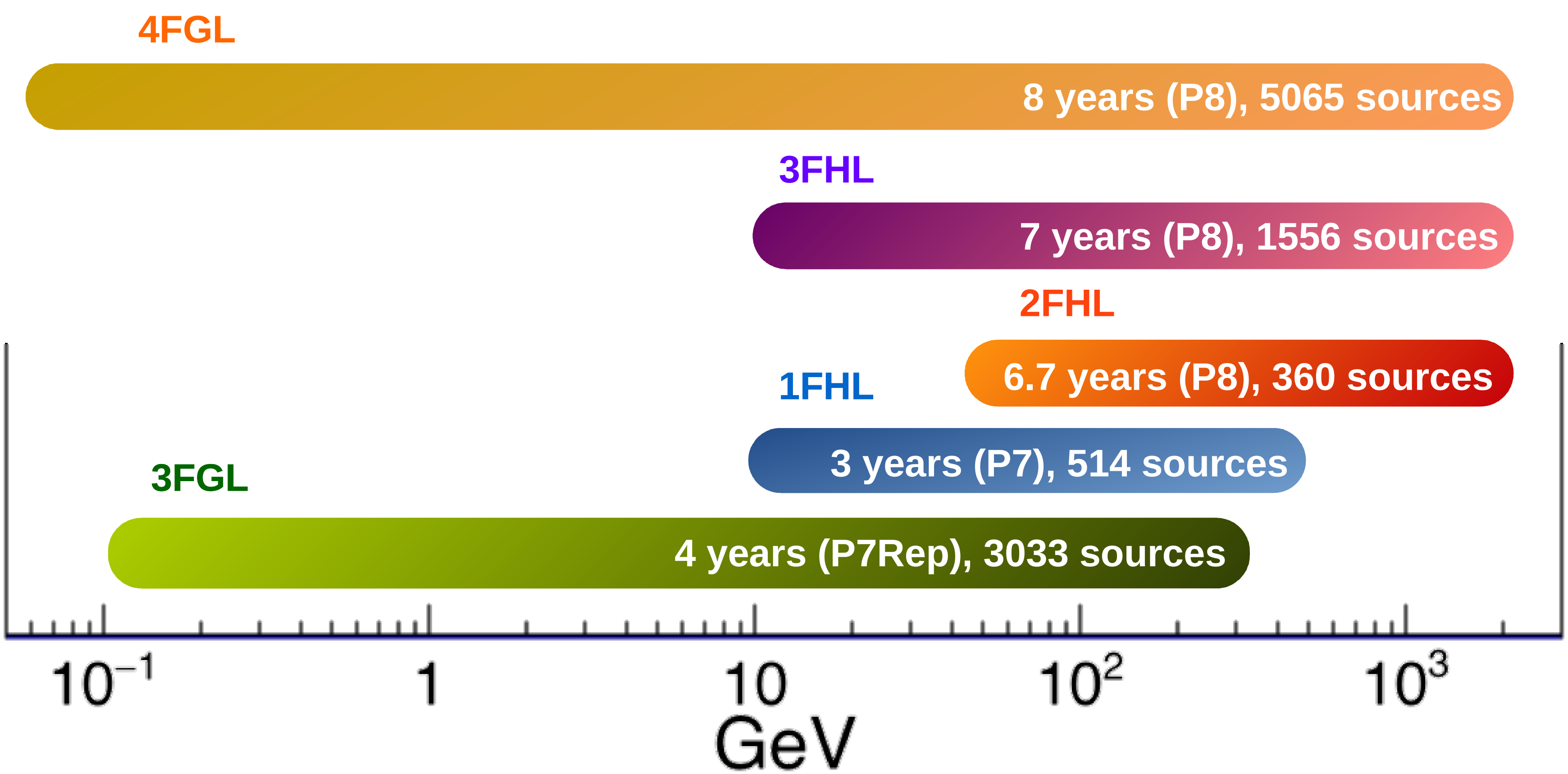

Blazars

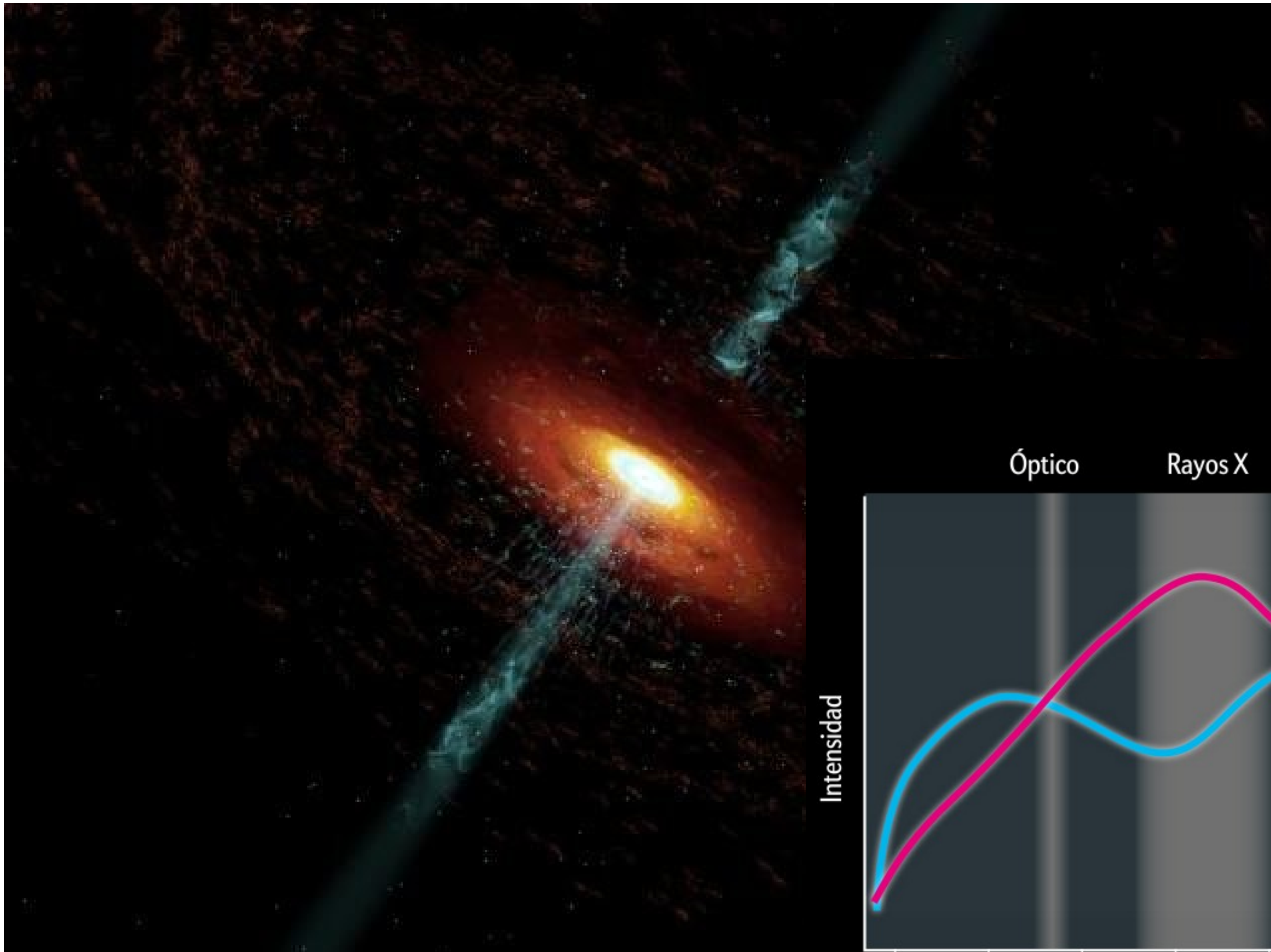

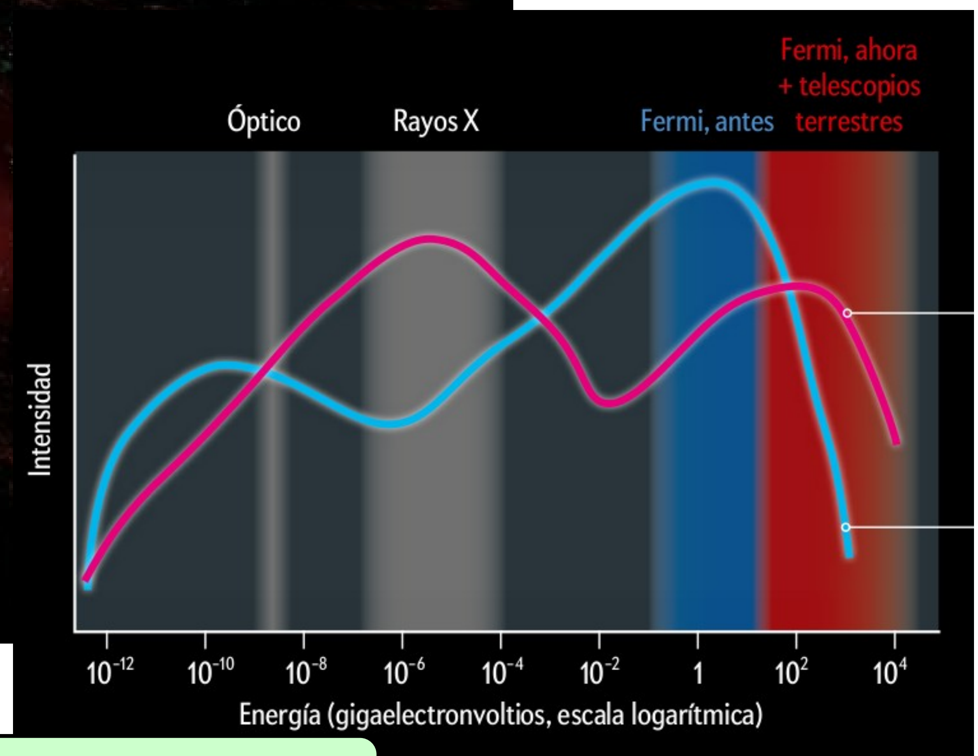

Emission described by homogeneous synchrotron/synchrotron-self Compton model.

Optical Depths from Gamma-ray Data

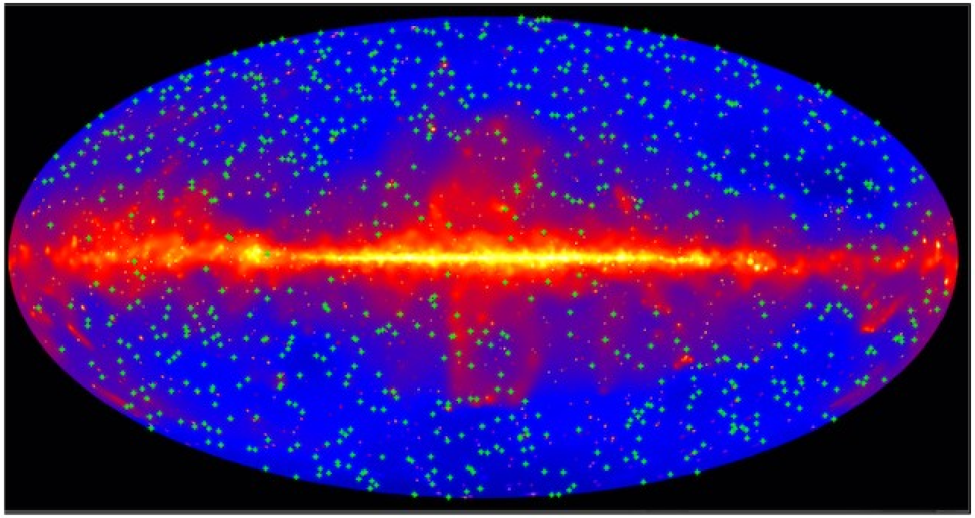

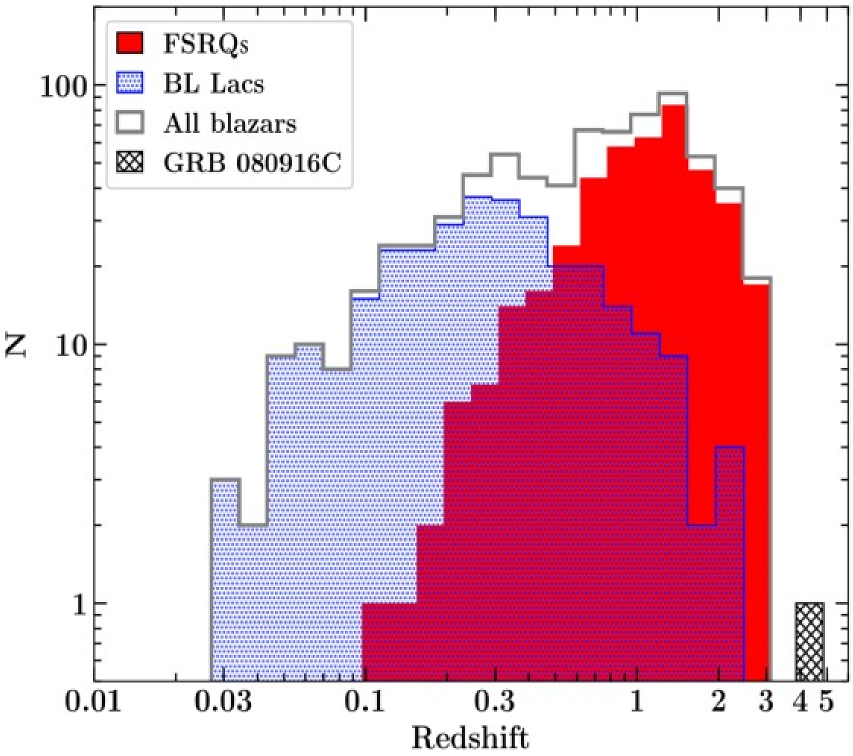

- Use 9 years of P8 LAT data
- 739 blazars + 1 GRB
- Perform a time-resolved analysis,
- Analysis optimized on simulations

Analysis improved over the Ackermann+12 results

Optical Depths from Gamma-ray Data

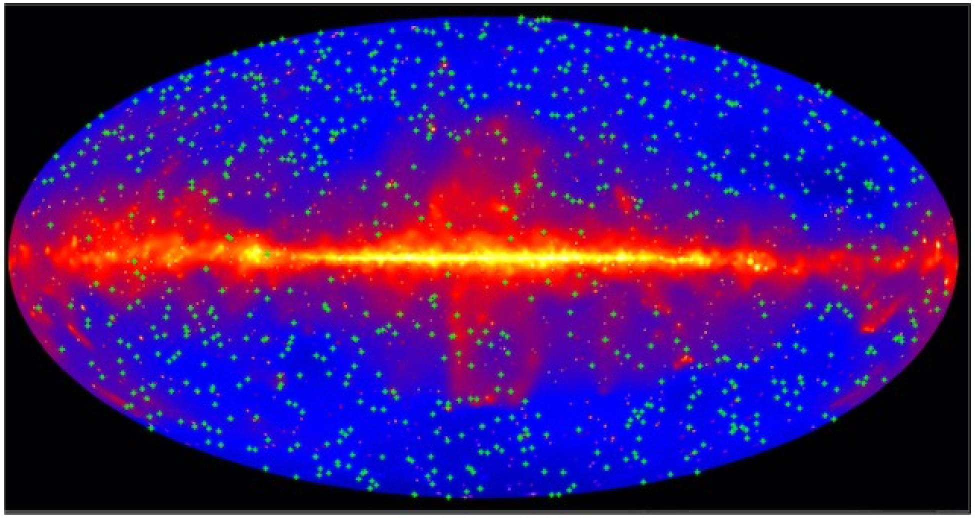

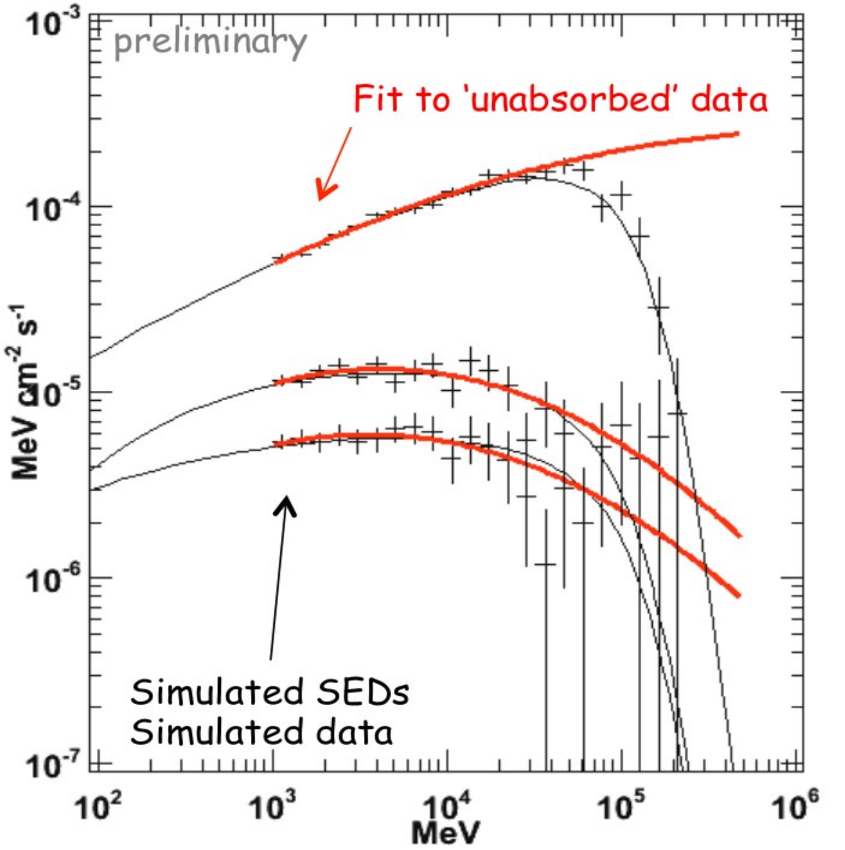

- Use 9 years of P8 LAT data
- 739 blazars + 1 GRB
- Perform a time-resolved analysis,
- Analysis optimized on simulations

$$F(E)_{absorbed} = F(E)_{intrinsic} \cdot e^{-b \cdot \tau_{model}}$$

Analysis improved over the Ackermann+12 results

Optical Depths from Gamma-ray Data

From detection (2012) to characterization (Now)

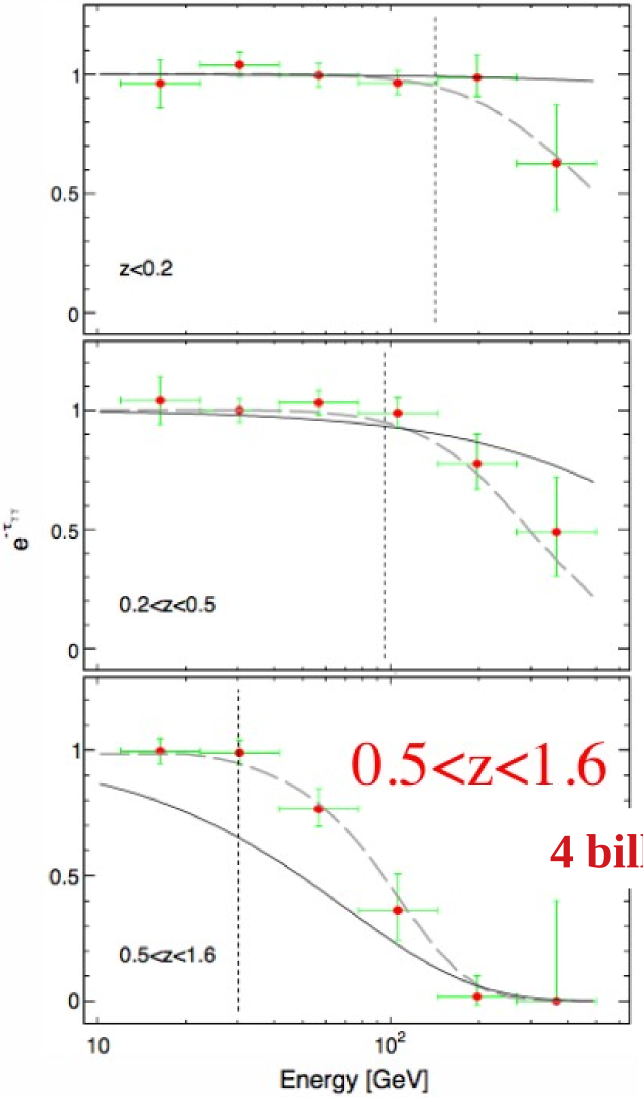

0.5<z<1.6

4 billion years

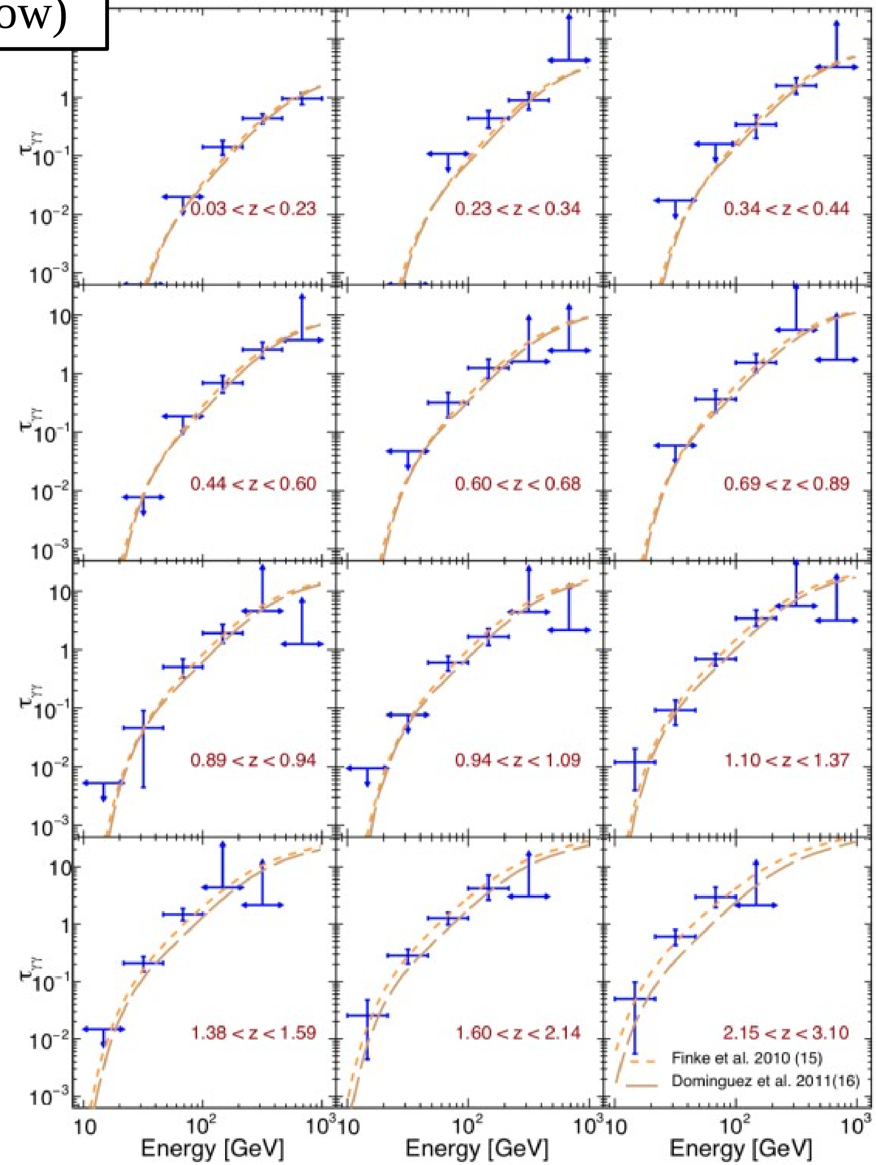

Cosmic Gamma-Ray Horizon

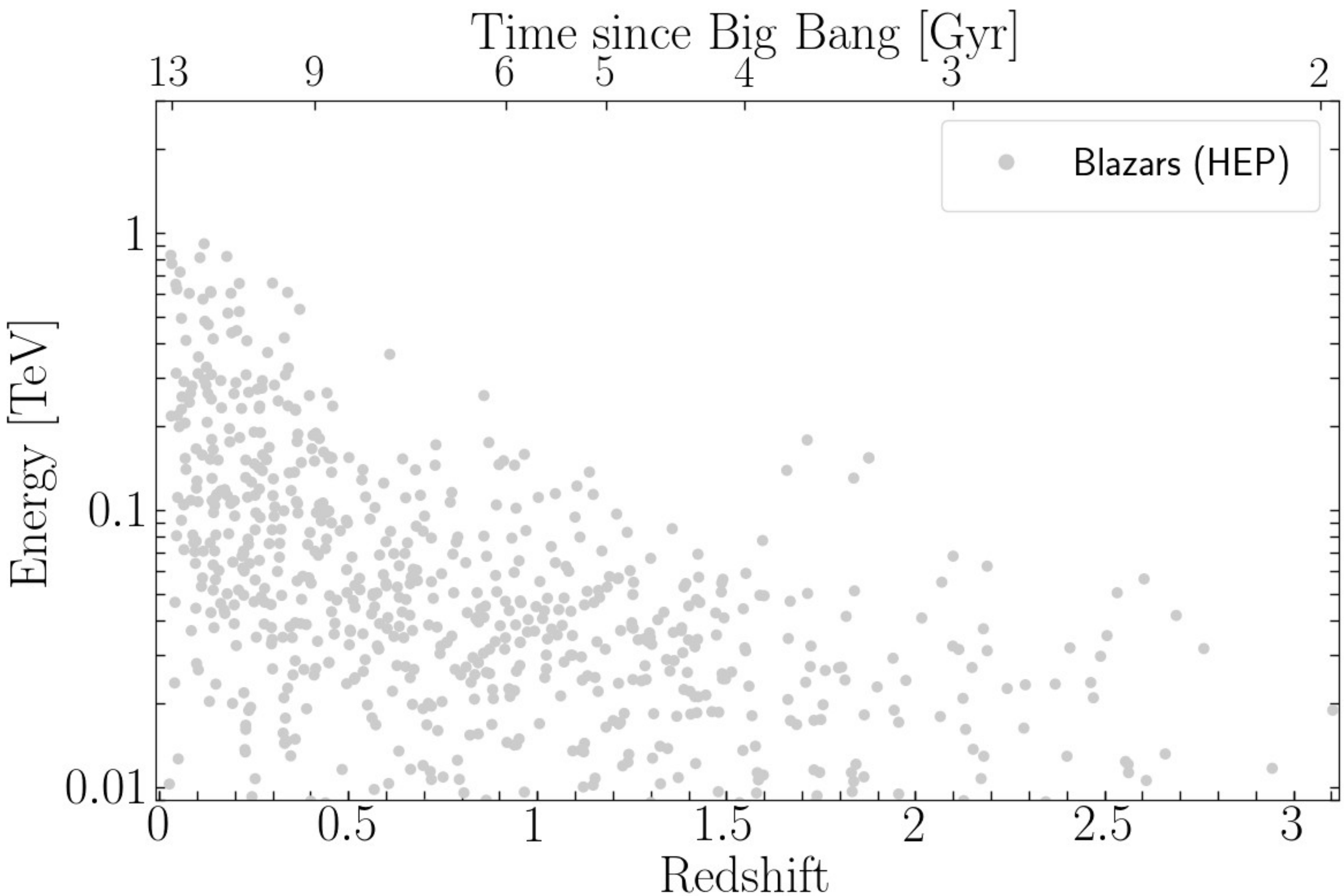

Cosmic Gamma-Ray Horizon

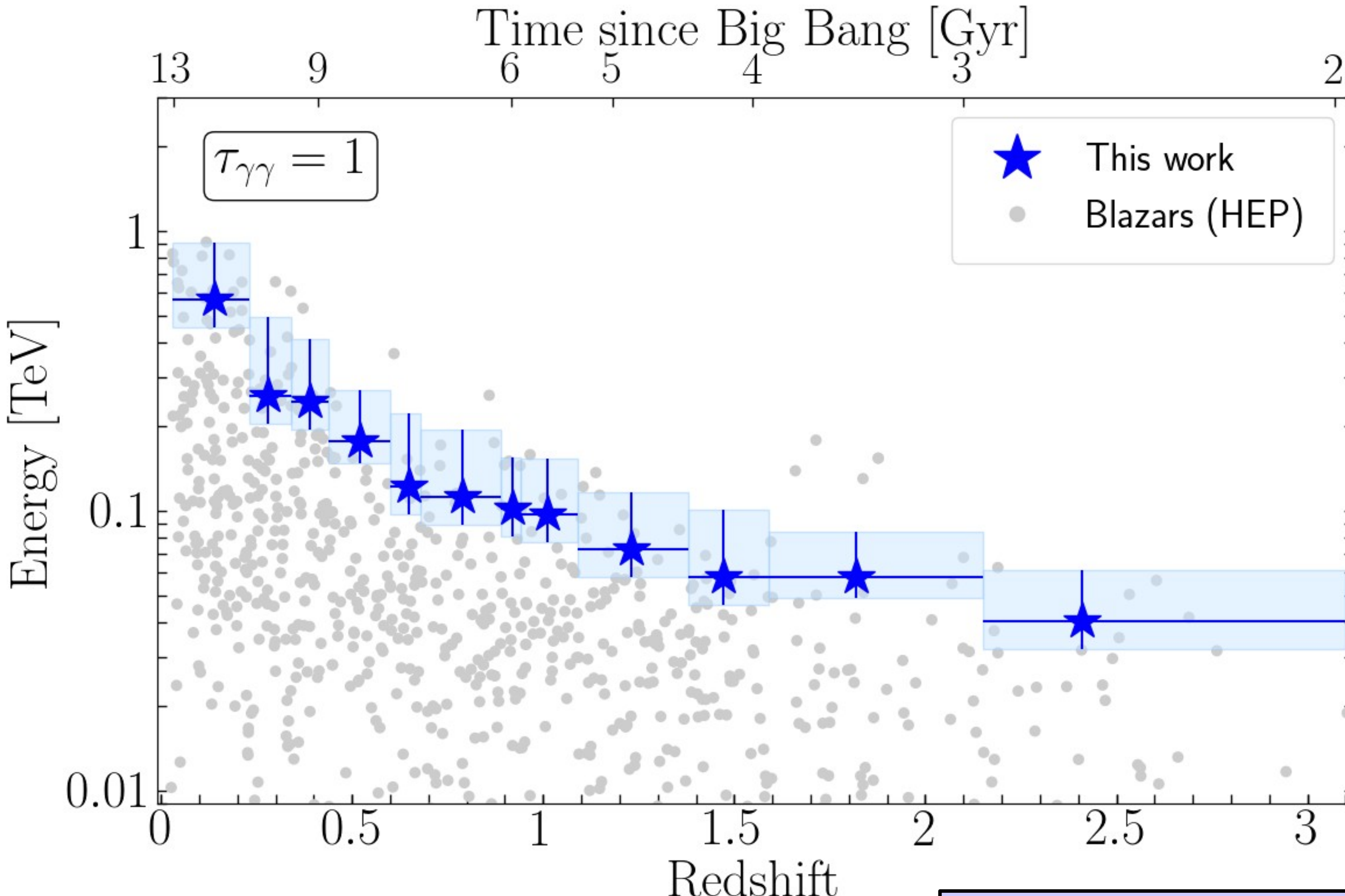

See also Fazio & Stecker 1970, Domínguez et al. 2013

Cosmic Gamma-Ray Horizon

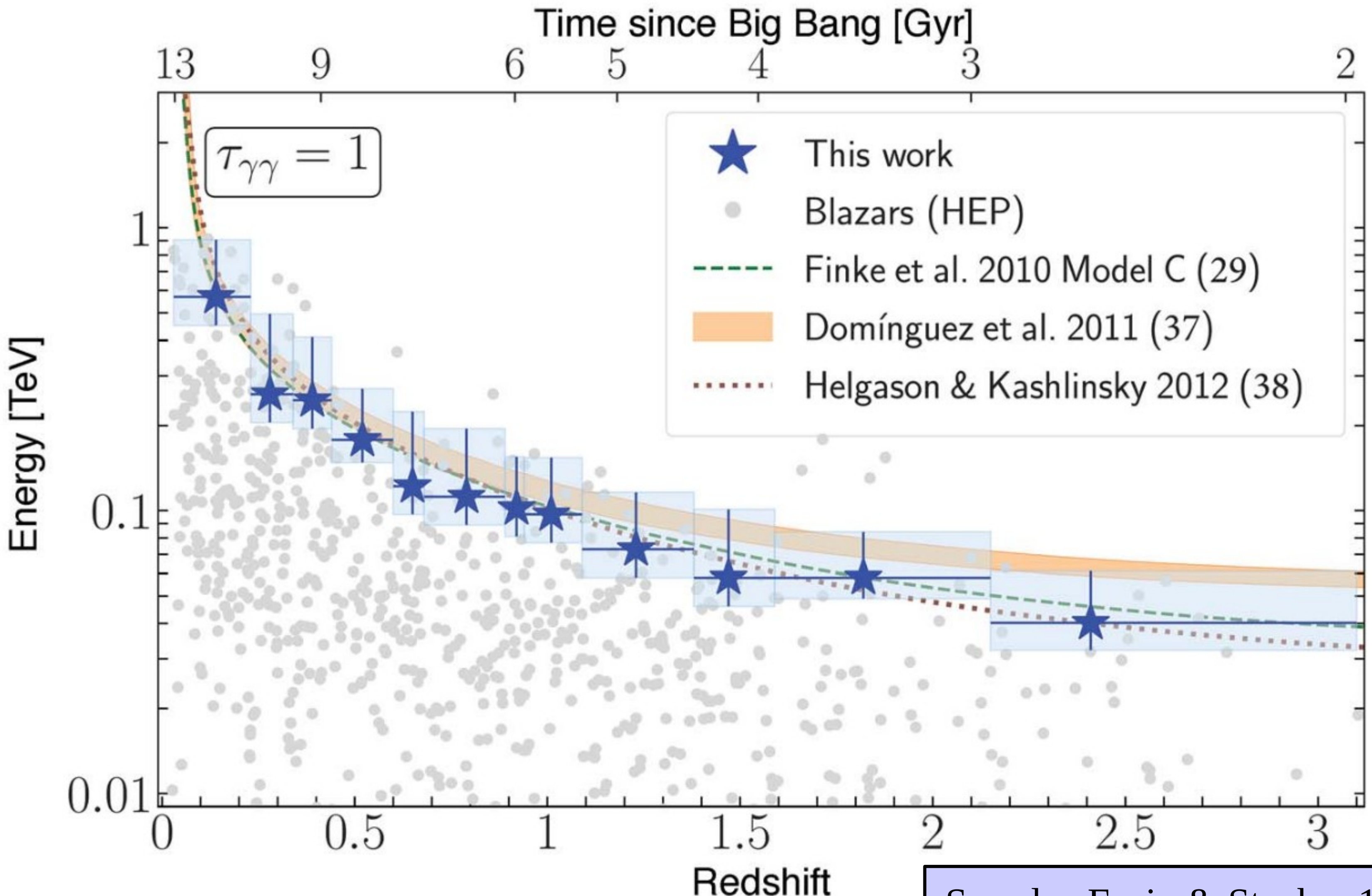

See also Fazio & Stecker 1970, Domínguez et al. 2013

Galaxy Luminosity Densities and EBL

$$n_{\mathrm{EBL}}(\epsilon, z) = (1+z)^3 \int_z^\infty \frac{j(\epsilon, z)}{\epsilon} \left| \frac{dt}{dz'} \right| dz'$$

$$j(\lambda_i, z) = \sum_i a_i \cdot \exp\left[-\frac{(\log \lambda - \log \lambda_i)^2}{2\sigma^2} \right] \times \frac{(1+z)^{b_i}}{1 + \left(\frac{1+z}{c_i} \right)^{d_i}},$$

Luminosity density evolution as sum of log-normal distributions that can evolve independently

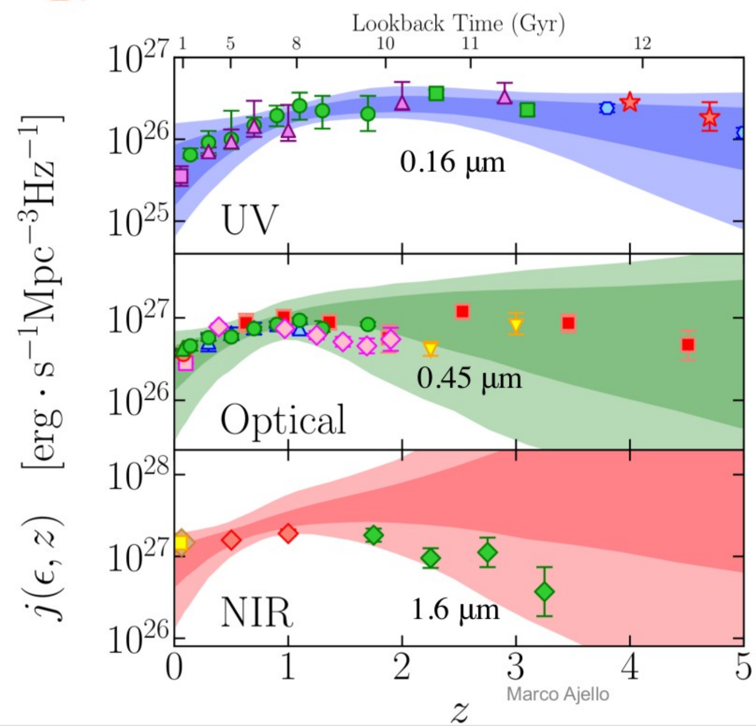

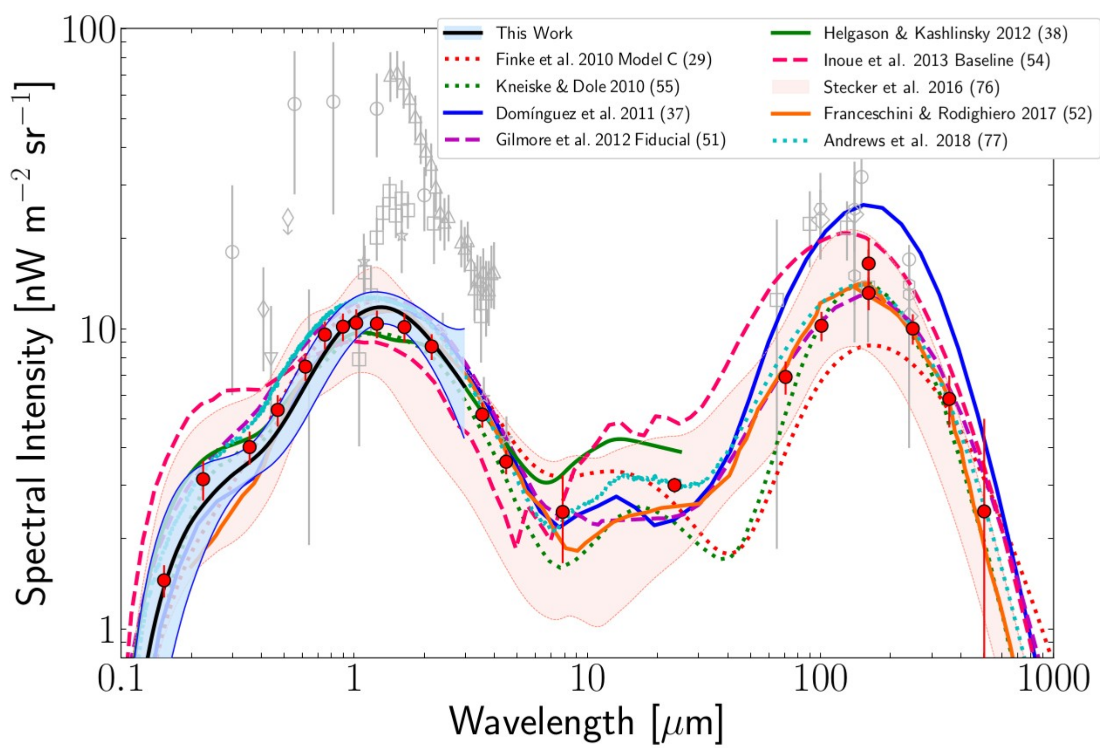

Galaxy Luminosity Densities and EBL

First EBL determination at *z*>0

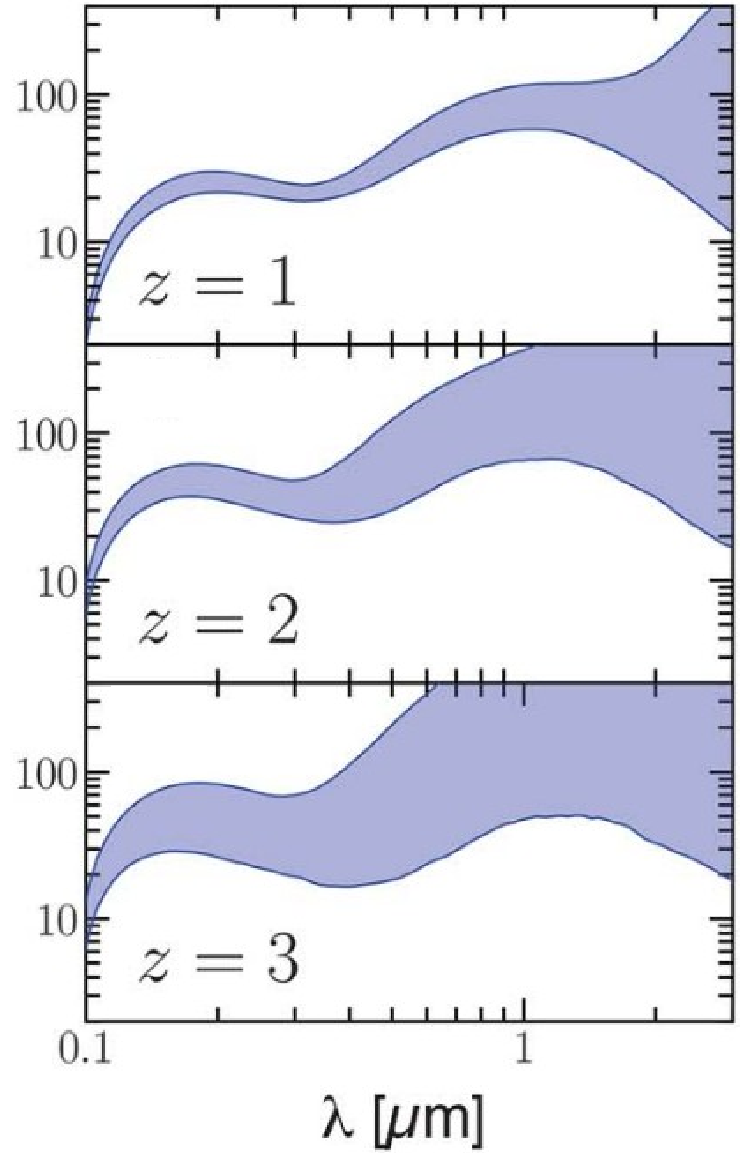

Cosmic Star Formation Rate

UV (0.16 microns) to SFR:

(1) Initial Mass Function

(2) Average Galaxy Extinction

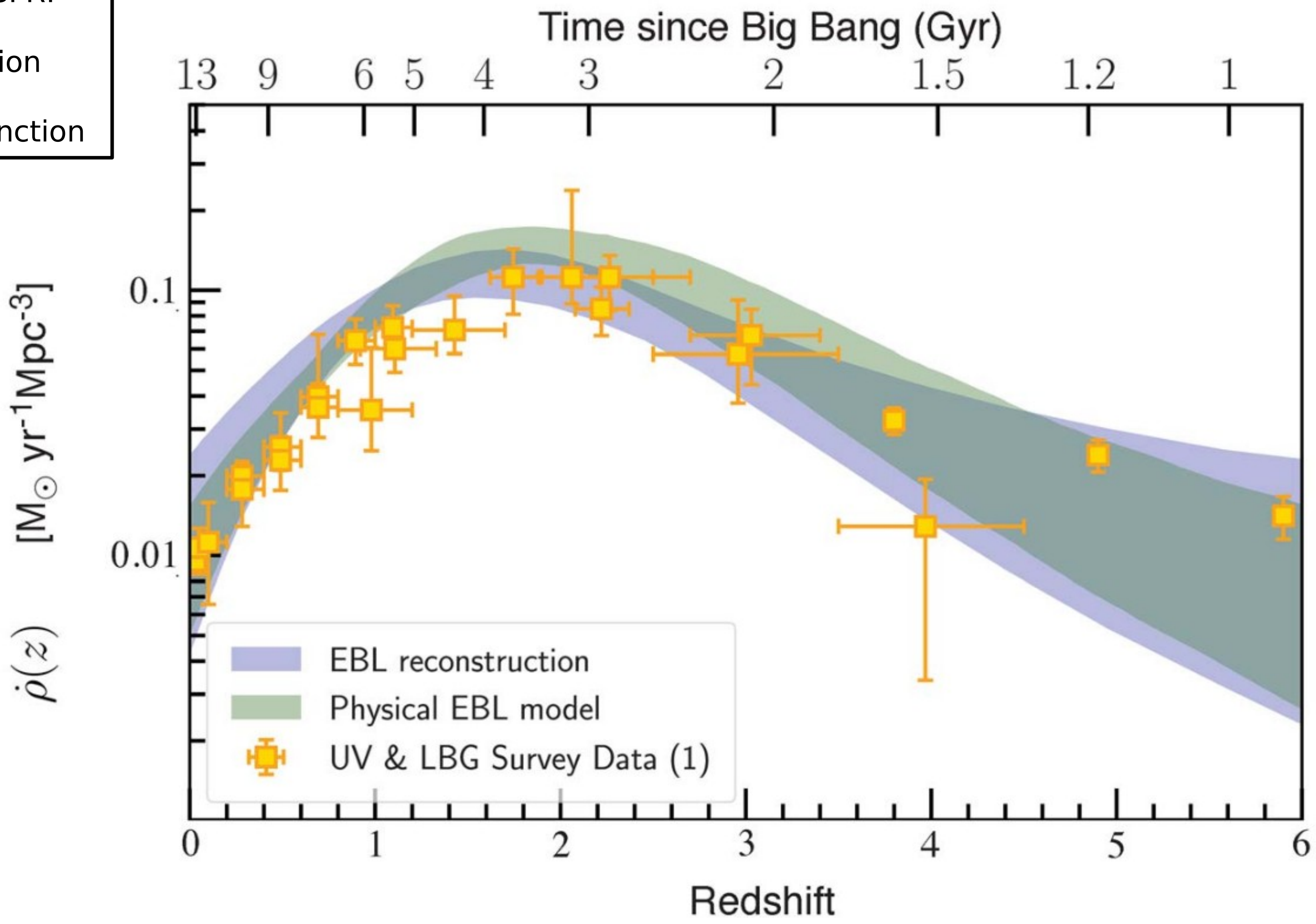

Re-ionization of the Universe

Hubble Frontier Fields

All deep blank-field HST data: Hubble Frontier Field Parallels, the XDF, CANDELS, and almost all other significant HST + ground-based probes

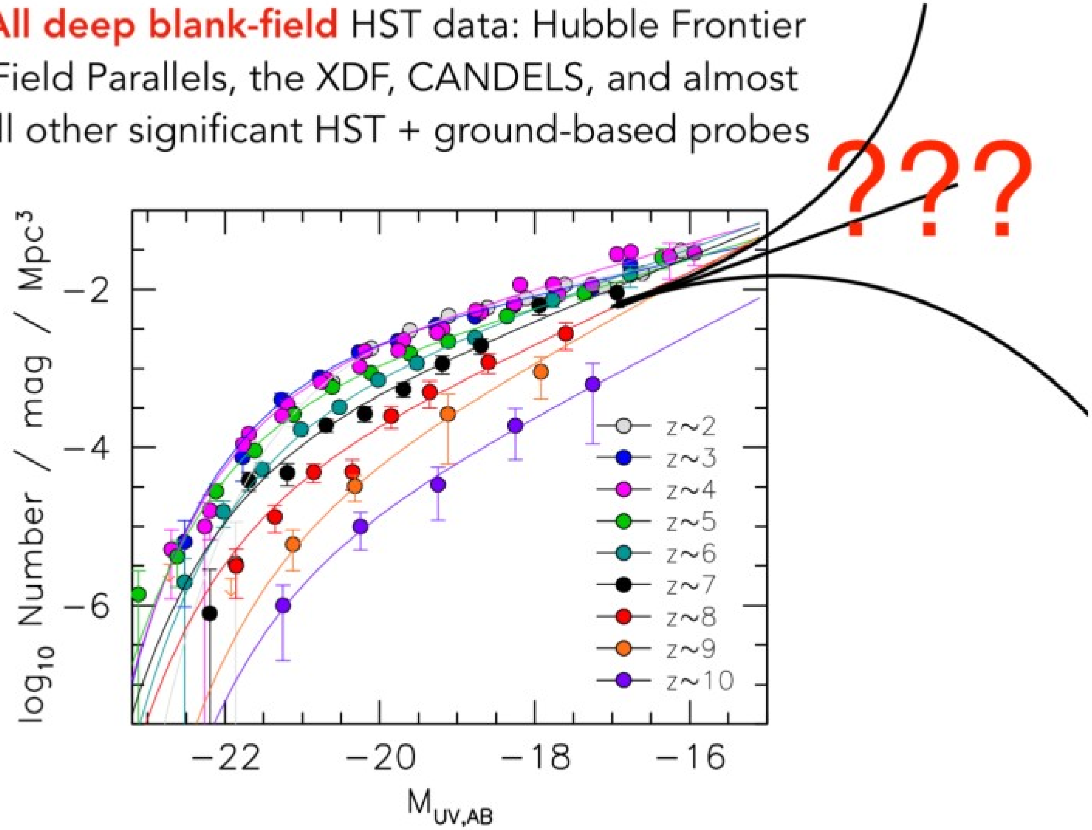

Bouwens+2018 (in prep); Oesch+2017

Re-ionization of the Universe

Hubble Frontier Fields

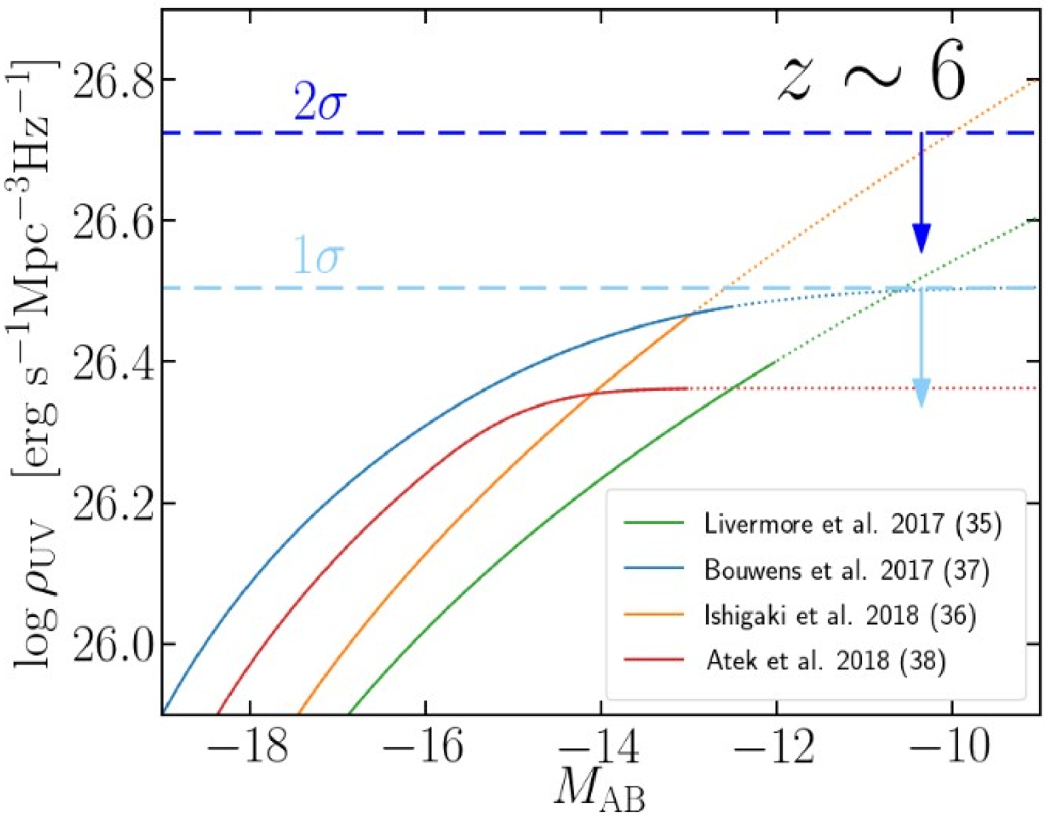

Constraints from gamma-ray attenuation

Optical Depths from Gamma-ray Data

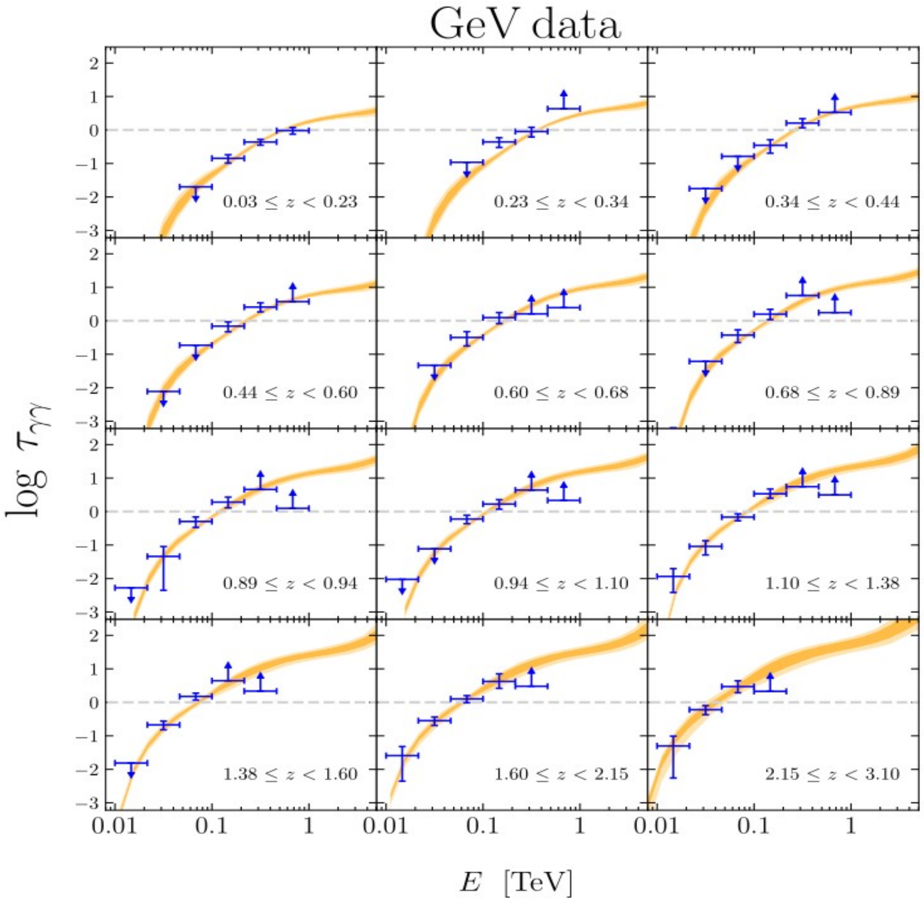

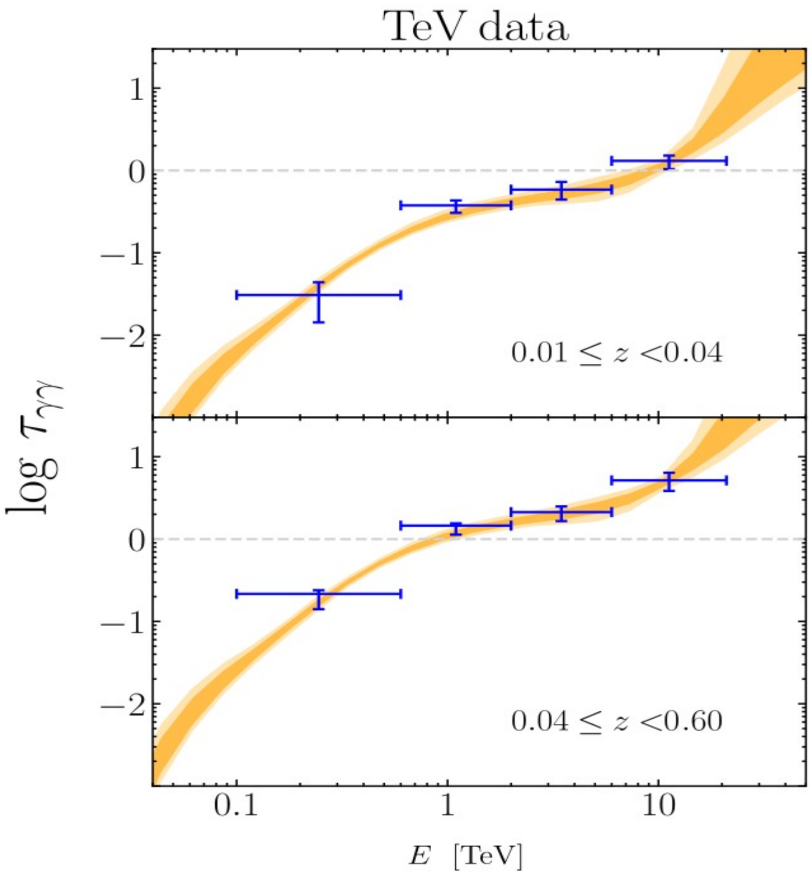

Extragalactic Background Light from Gamma Rays

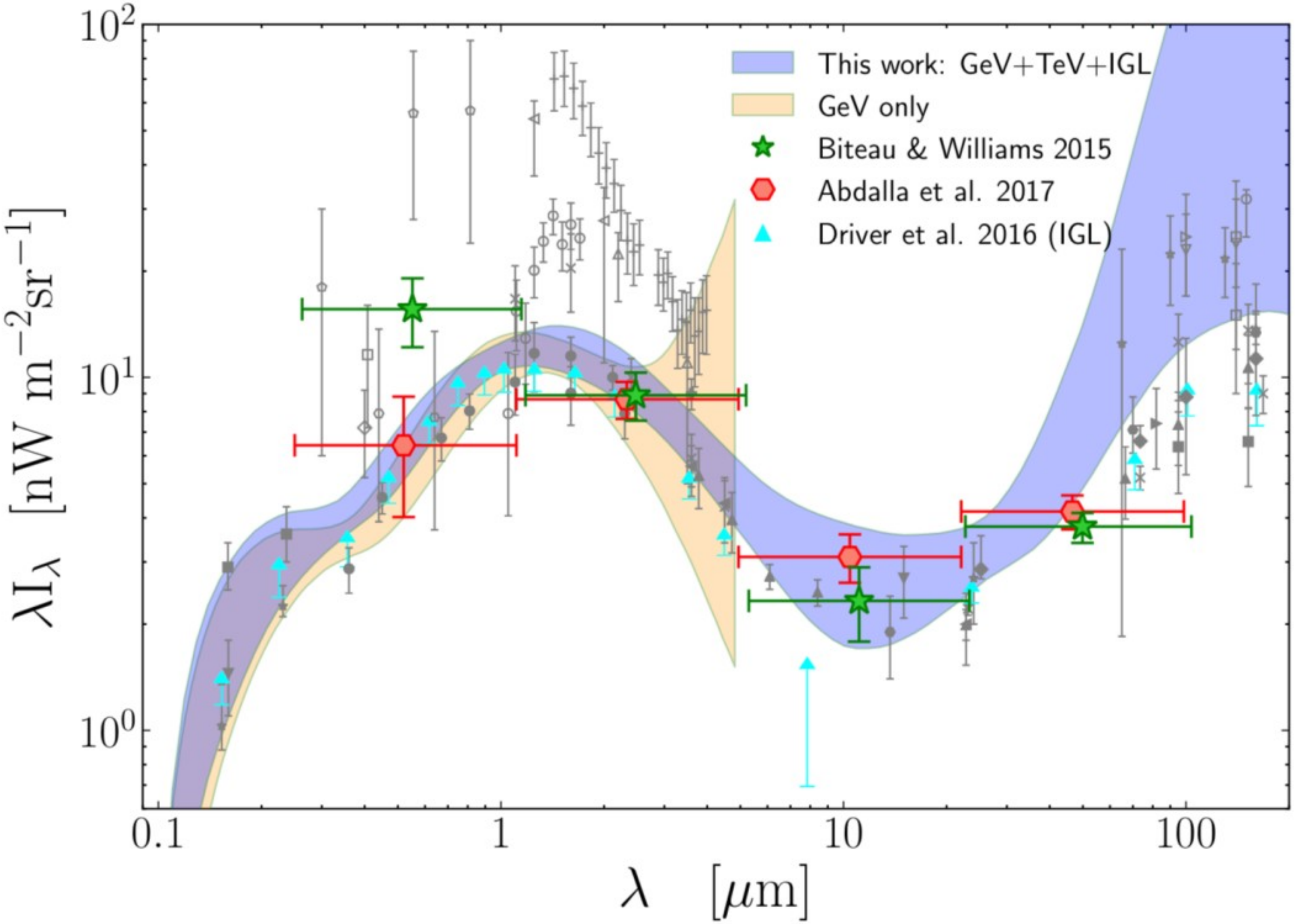

Local Extragalactic Background Light
(also see works by the MAGIC, VERITAS, and H.E.S.S. Collaborations)

Tension on H_0 Measurements

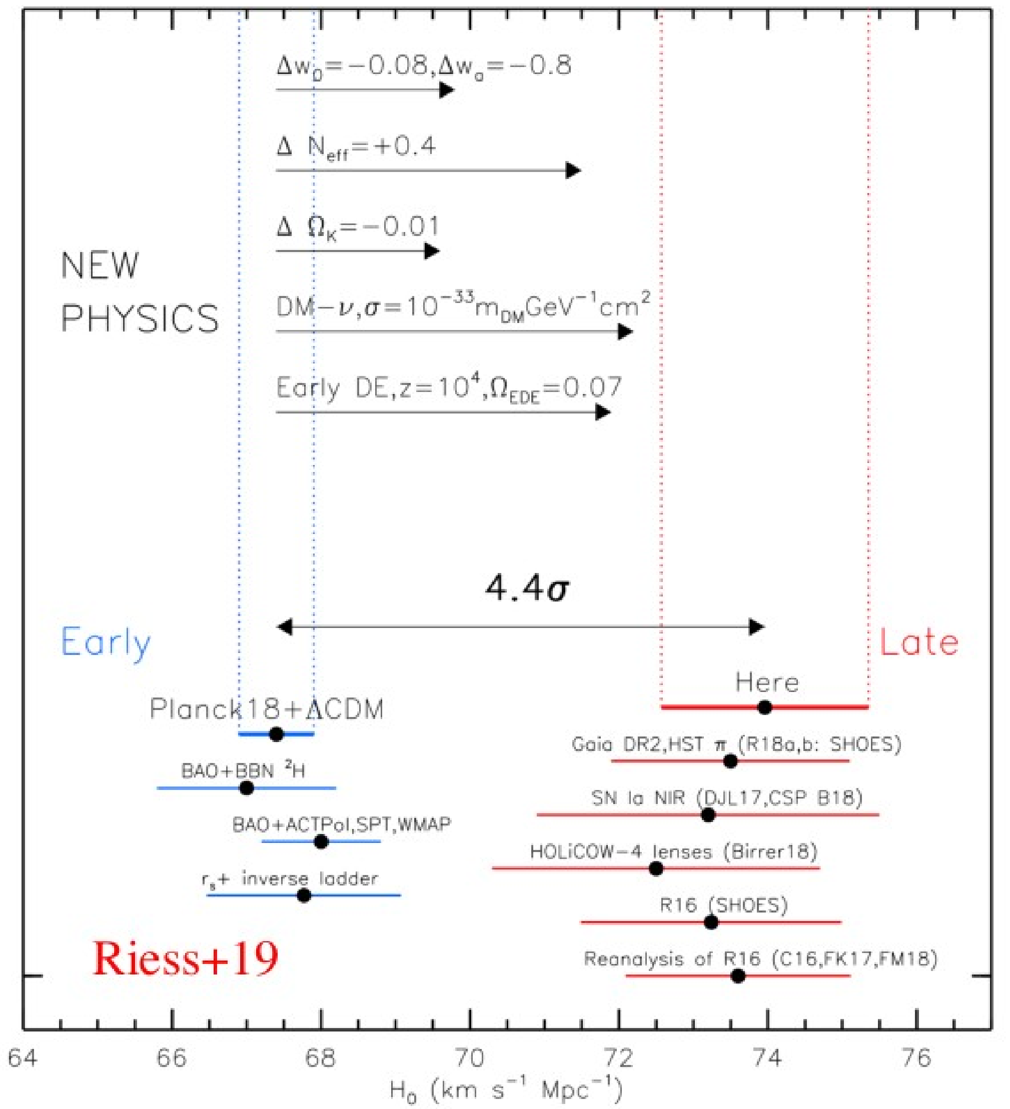

Gamma-ray Attenuation

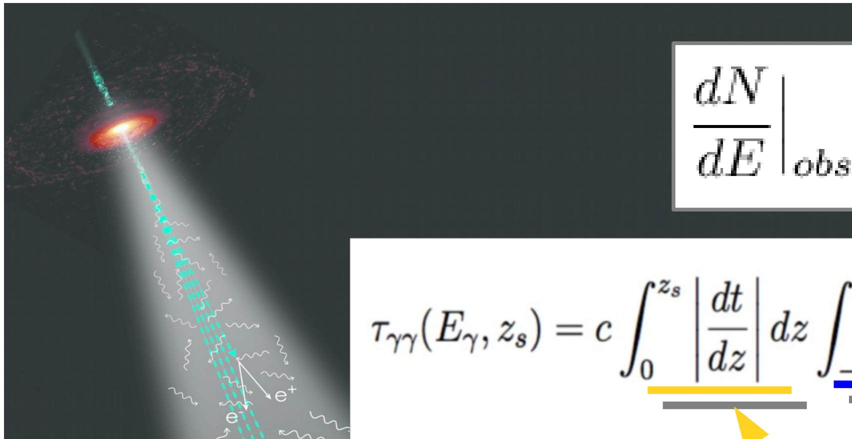

$$\frac{dN}{dE}\bigg|_{obs} = \frac{dN}{dE}\bigg|_{int} \exp\left[-\tau(E,z)\right]$$

$$\tau_{\gamma\gamma}(E_\gamma, z_s) = c\int_0^{z_s}\left|\frac{dt}{dz}\right| dz \int_{-1}^{1}(1-\mu)\frac{d\mu}{2}\int_{2m_e^2c^4/\epsilon_\gamma(1-\mu)}^{\infty}\sigma(\epsilon_{\mathrm{EBL}},\epsilon_\gamma,\mu)\, n_{\mathrm{EBL}}(\epsilon,z)\, d\epsilon_{\mathrm{EBL}}$$

$$n_{\mathrm{EBL}}(\epsilon,z) = (1+z)^3\int_z^{\infty}\frac{j(\epsilon,z)}{\epsilon}\left|\frac{dt}{dz'}\right| dz'$$

distance

cross section

EBL photon density evolution

See Domínguez & Prada 13,
Biteau & Williams 15

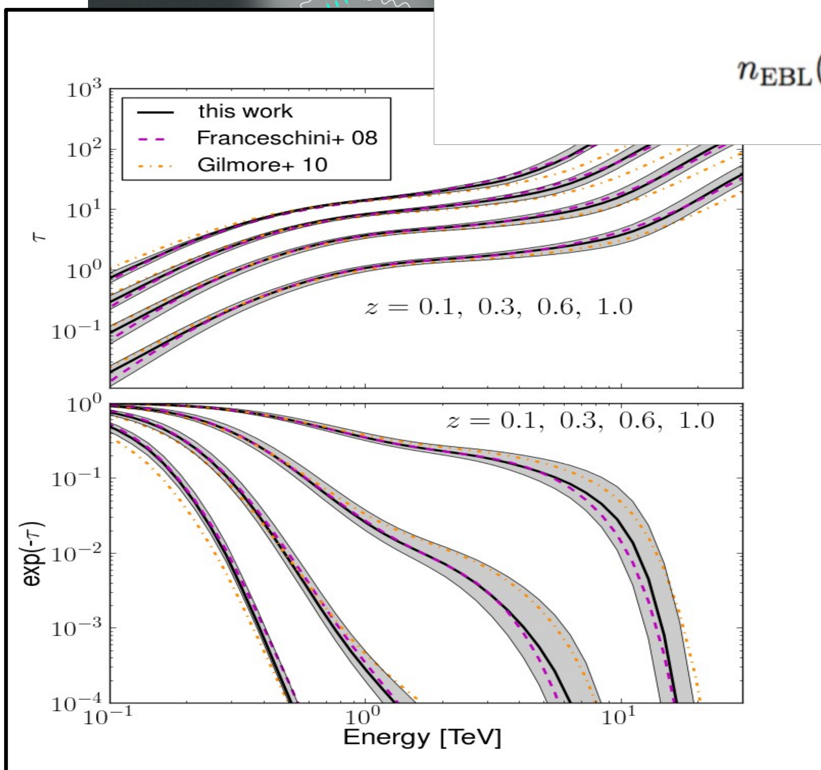

: Nina McCurdy & Joel Primack

Measuring H_0 with Gamma-ray Attenuation

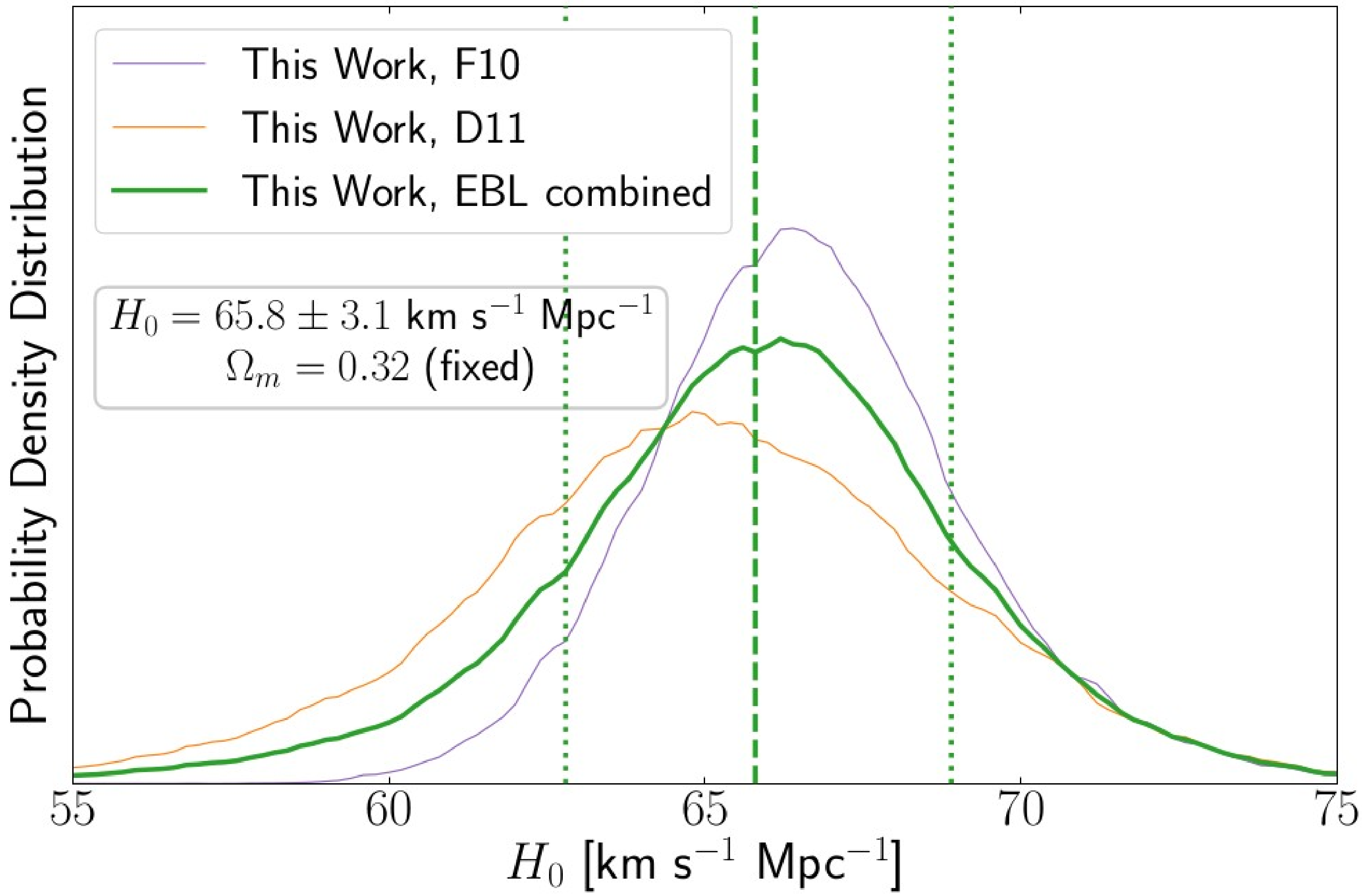

Tension on H_0 Measurements

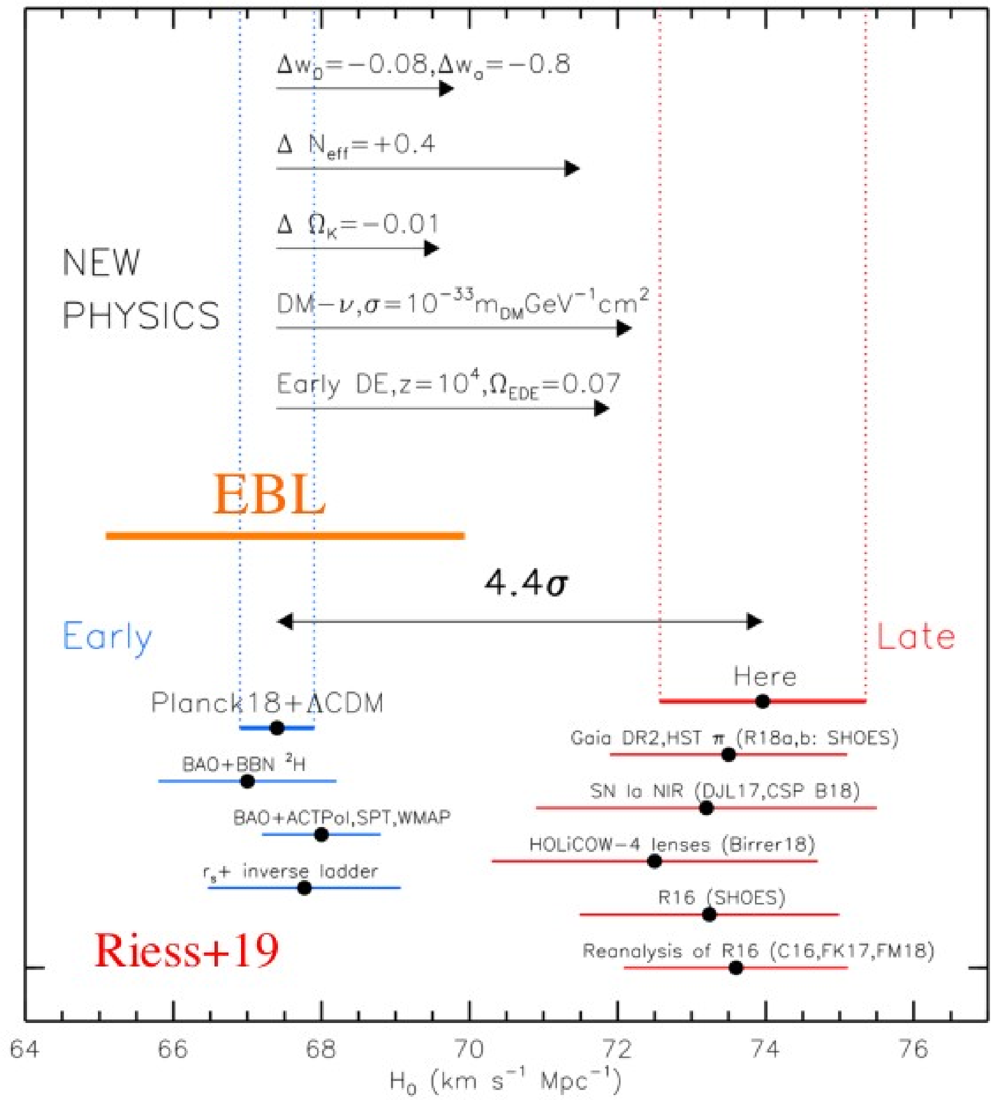

Measuring H_0 and Ω_m with Gamma-ray Attenuation

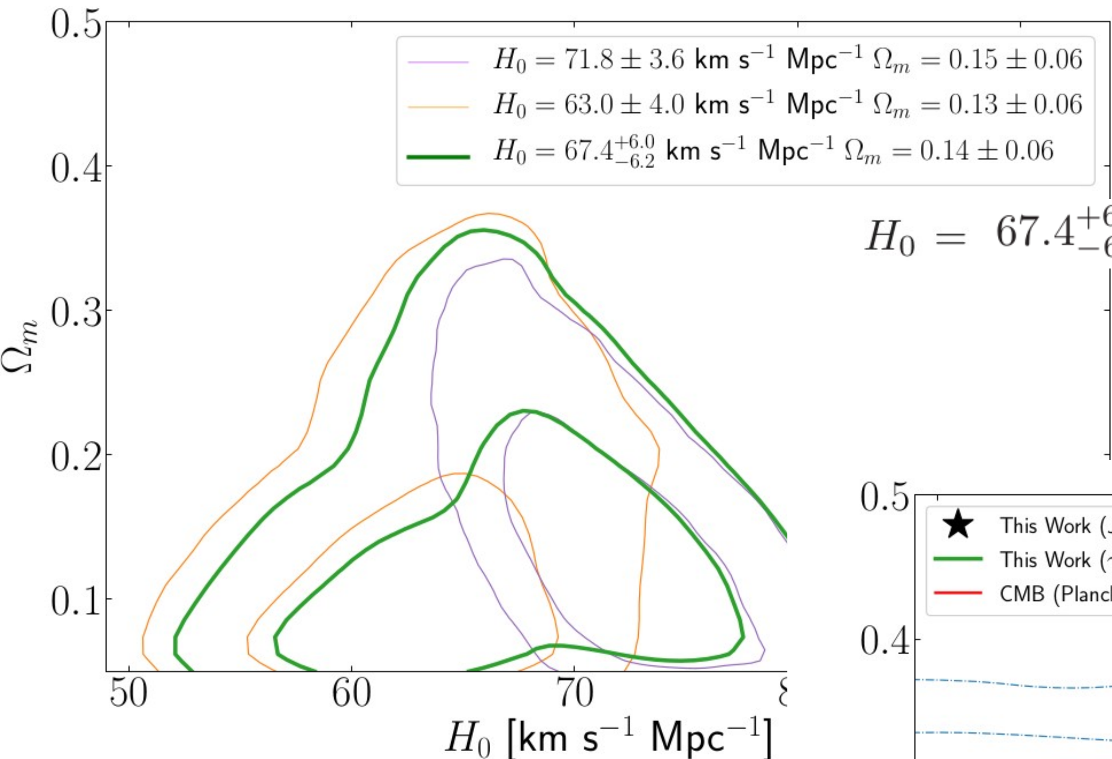

$$H_0 = 67.4^{+6.0}_{-6.2} \text{ km s}^{-1} \text{ Mpc}^{-1} \text{ and } \Omega_m = 0.14^{+0.06}_{-0.07}$$

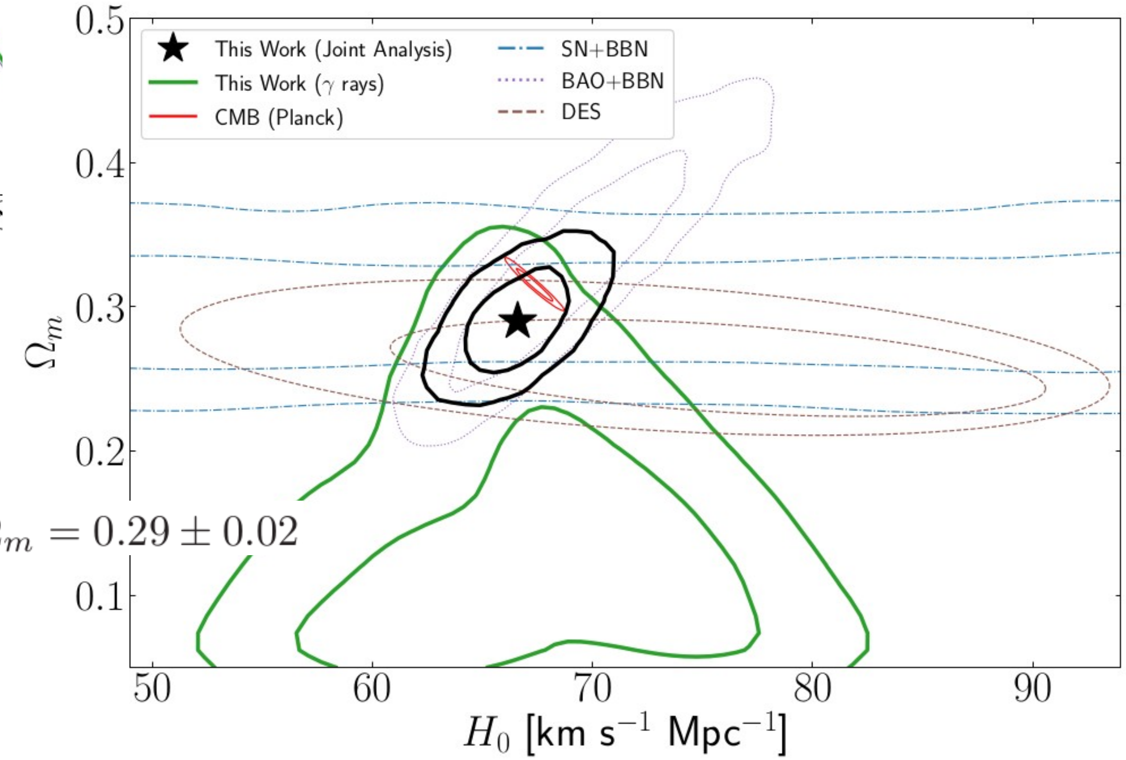

$$H_0 = 66.6 \pm 1.6 \text{ km s}^{-1} \text{ Mpc}^{-1} \text{ and } \Omega_m = 0.29 \pm 0.02$$

Take Home Messages

1.- Very significant detection and characterization of the EBL attenuation up to z~3.

2.- Complete derivation so far of the local EBL and its evolution over redshift from *Fermi*-LAT and Cherenkov data.

3.- Derived Cosmic Star formation Rate Density up to z~5 unbiased from different galaxy survey incompleteness.

4.- Cosmological measurement of H_0 and Ω_m from our independent technique.

Gamma-ray astronomy has matured enough and is providing useful measurements in galaxy evolution and cosmology

Backup

Cosmology Dependence on the Optical Depth

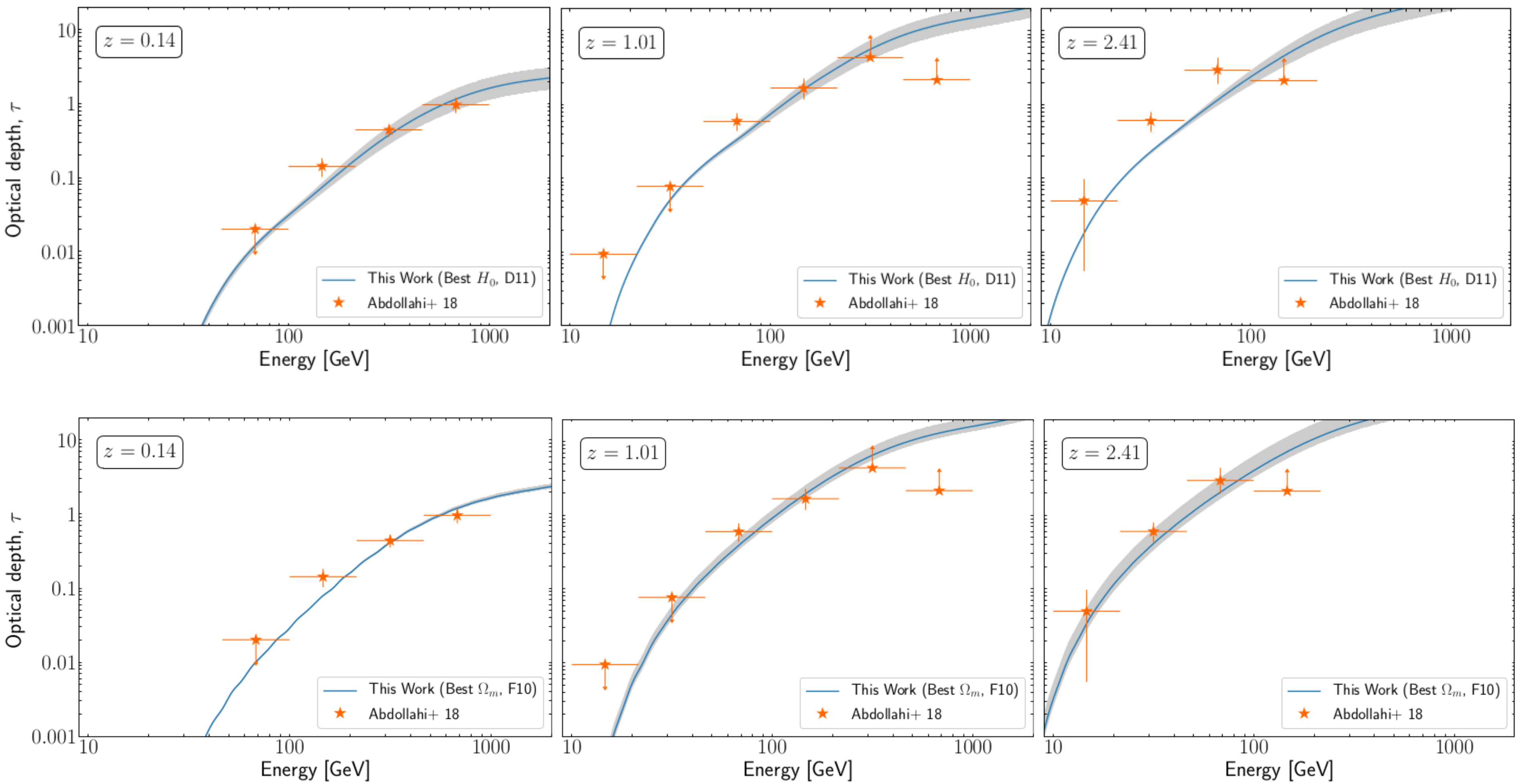

Comparison with other Methodologies

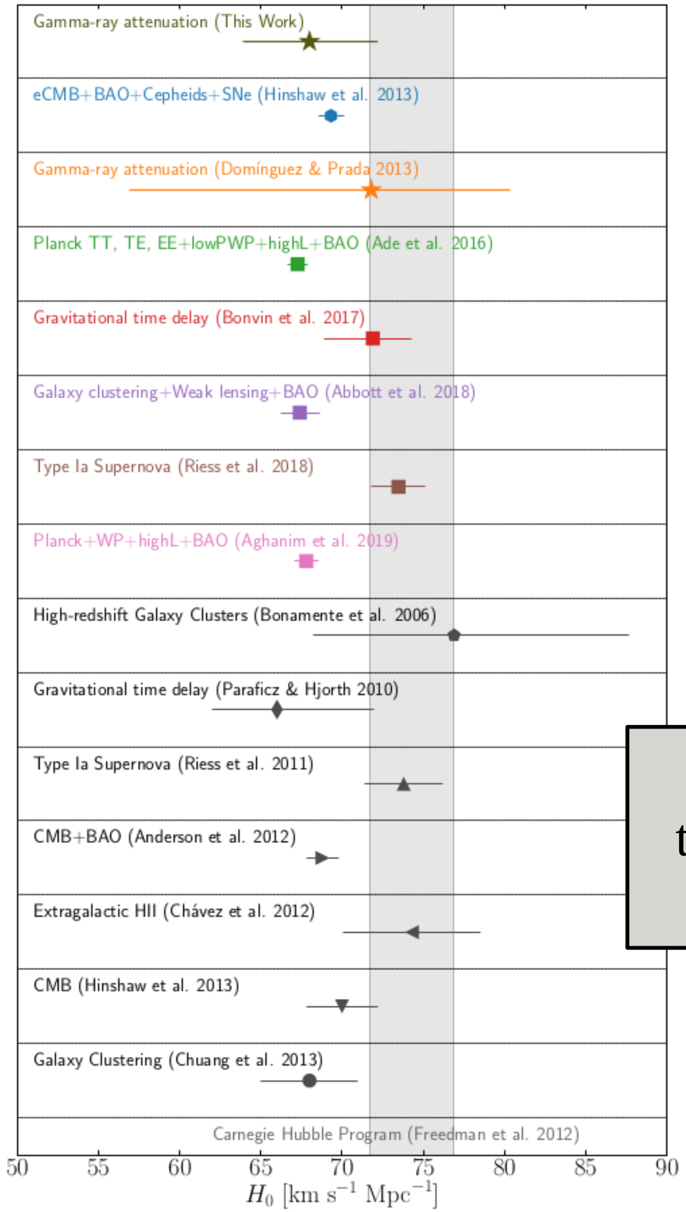

Combination of techniques is important to control systematics

EBL models: Finke+ 10

Dust absorption

IMF

Stellar photons

Stellar emissivity (luminosity density):

$$\epsilon\, j_\epsilon^{stars}(z) = m_e c^2 \epsilon^2 \frac{dN}{dt\, d\epsilon\, dV} = \epsilon^2 f_{esc}(\epsilon) \int_{m_{min}}^{m_{max}} dm\, \xi(m)\, \dot{N}_*(\epsilon; m, t_*(z)) \times \int_z^{z_{max}} dz_1 \left|\frac{dt_*}{dz_1}\right| \psi(z_1) .$$

SFR

Expansion of universe

Stellar parameters from Eggleton et al. (1989), ApJ, 347, 998
Dust absorption: Driver et al. (2008), ApJ, 678, L101

Dust emission computed self-consistently:

$$f_n \int d\epsilon\, \frac{1}{f_{esc}(\epsilon)} [1 - f_{esc}(\epsilon)]\, j_\epsilon^{stars}(z) = \int d\epsilon\, j_{\epsilon,n}(\Theta_n)$$

Three component dust model:

Component	n	f_n	T_n [K]	Θ_n [10^{-9}]
Warm Large Grains	1	0.60	40	7
Hot Small Grains	2	0.05	70	12
PAHs	3	0.35	450	76

EBL energy density: $$\epsilon\, u_{EBL}(\epsilon; z) = \int_z^{z_{max}} dz_1\, \frac{\epsilon'' j_{\epsilon''}(z_1)}{(1+z_1)} \left|\frac{dt_*}{dz_1}\right|$$

JF, Razzaque, & Dermer, (2010), ApJ, 712, 238
Razzaque, Dermer, & JF, (2009), ApJ, 697, 483

EBL models: Domínguez+ 11

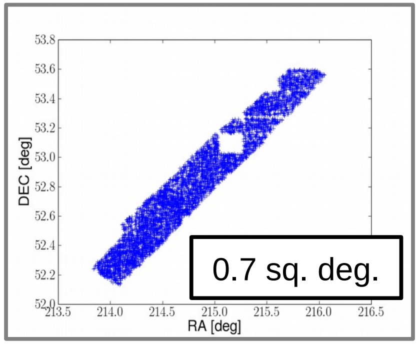

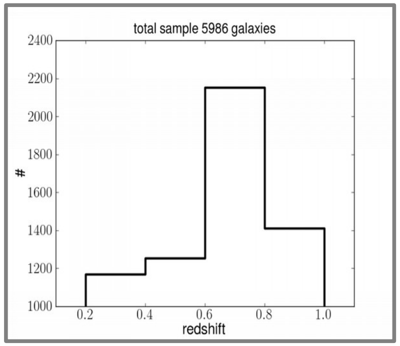

EGS field

Band	λ_{eff} [μm]	Observatory	Req.	UL [μJy]
FUV	0.1539	GALEX	ext	-
NUV	0.2316	GALEX	ext	-
B	0.4389	CFHT12K	det	-
R	0.6601	CFHT12K	det	-
I	0.8133	CFHT12K	det	-
K_S	2.14	WIRC	det	-
IRAC 1	3.6	IRAC	det	-
IRAC 2	4.5	IRAC	obs	1.2
IRAC 3	5.8	IRAC	obs	6.3
IRAC 4	8.0	IRAC	obs	6.9
MIPS 24	23.7	MIPS	obs	30

Total: 5986 galaxies

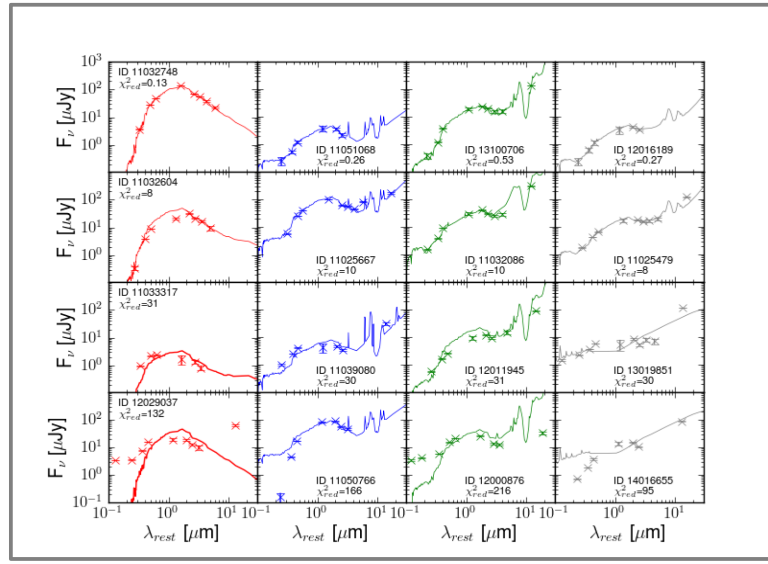

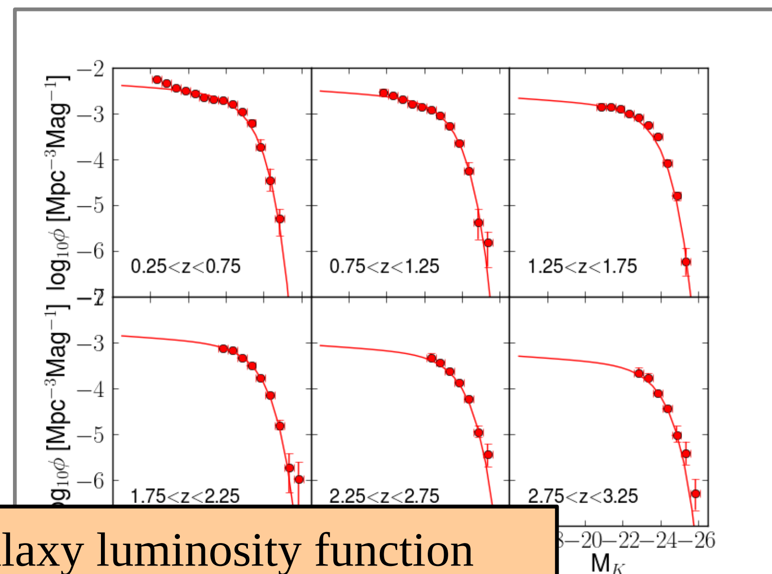

Galaxy luminosity function
rest-frame K-band, Cirasuolo+ 10